1 **Extracellular vesicles regulate yeast growth, biofilm formation, and yeast-to-hypha**

2 **differentiation in *Candida albicans***

3

4 **Running title: Populational functions of fungal EVs**

5

6 Leandro Honorato[1]*, Joana Feital Demetrio[1]*, Cameron C. Ellis[2], Alicia Piffer[1], Yan

7 Pereira[1], Susana Frases[3], Glauber Ribeiro de Sousa Araújo[3], Bruno Pontes[4], Maria Tays

8 Mendes[2,#], Marcos Dias Pereira[5], Allan J. Guimarães[6], Natalia Martins da Silva[1], Gabriele

9 Vargas[1], Luna Joffe[7], Maurizio Del Poeta[7,8], Joshua D. Nosanchuk[9], Daniel Zamith[9], Flavia

10 Coelho Garcia dos Reis[10,11], Marcio L. Rodrigues[10,12] Sharon de Toledo Martins[10], Lysangela

11 Ronalte Alves[10], Igor C. Almeida[2], and Leonardo Nimrichter[1]

12

13 [1] Laboratório de Glicobiologia de Eucariotos, Departamento de Microbiologia Geral, Instituto

14 de Microbiologia, Universidade Federal do Rio de Janeiro, Brasil

15 [2] Department of Biological Sciences, Border Biomedical Research Center, University of Texas

16 at El Paso, El Paso, Texas, United States of America

17 [3] Laboratório de Ultraestrutura Celular Hertha Meyer, Instituto de Biofísica Carlos Chagas

18 Filhos (IBCCF) Universidade Federal do Rio de Janeiro, Brazil

19 [4] LPO-COPEA, Instituto de Ciências Biomédicas & Centro Nacional de Biologia Estrutural e

20 Bioimagem (CENABIO), Universidade Federal do Rio de Janeiro, Brazil

21 [5] Laboratório de Citotoxicidade e Genotoxicidade, Departamento de Bioquímica, Instituto de

22 Química, Universidade Federal do Rio de Janeiro, Brazil

23 [6] Laboratório de Bioquímica e Imunologia das Micoses, Departamento de Microbiologia e

24 Parasitologia, Instituto Biomédico, Universidade Federal Fluminense, Brazil

1   [7] Department of Microbiology and Immunology, Stony Brook University, Stony Brook, NY,

2   USA

3   [8] Department of Microbiology and Immunology and Division of Infectious Diseases, Stony

4   Brook University, Stony Brook, NY, USA; Veterans Affairs Medical Center, Northport, NY,

5   USA.

6   [9] Department of Microbiology and Immunology, Albert Einstein College of Medicine, Bronx,

7   NY, USA; Division of Infectious Diseases, Department of Medicine, Albert Einstein College

8   of Medicine, Bronx, NY, USA.

9   [10] Instituto Carlos Chagas (ICC), Fundação Oswaldo Cruz (FIOCRUZ), Curitiba, Brasil

10 [11] Centro de Desenvolvimento Tecnológico em Saúde (CDTS), Fundação Oswaldo Cruz, Rio

11 de Janeiro, Brazil

12 [12] Instituto de Microbiologia Paulo de Góes, Universidade Federal do Rio de Janeiro, Brazil

13 [13] Gene Expression Regulation Laboratory, Carlos Chagas Institute, Fiocruz PR, Brazil

14

15 * These authors contributed equally to this work.

16 [#] Current address: Department of Microbiology and Immunology, University of Maryland

17 School of Medicine, 685 W. Baltimore St. HSF I, room 356, Baltimore, MD, 21201, USA

18

1   **Abstract**

2   The ability to undergo morphological changes during adaptation to distinct

3   environments is exploited by *Candida albicans* and has a direct impact on virulence. In this

4   study, we investigated the influence of fungal extracellular vesicles (EVs) during yeast

5   growth, biofilm formation, and morphogenesis in *C. albicans*. Addition of *C. albicans* EVs

6   (*Ca* EVs) to the culture medium positively affected yeast growth. Using crystal violet

7   staining and scanning electron microscopy (SEM), we demonstrated that *Ca* EVs inhibited

8   biofilm formation by *C. albicans in vitro*. By time-lapse microscopy and SEM, we showed

9   that *Ca* EV-treatment stops filamentation promoting pseudohyphae formation with multiple

10   sites for yeast budding. The ability of *Ca* EVs to regulate dimorphism was further compared

11   to EVs isolated from different *C. albicans* strains, *Saccharomyces cerevisiae*, and

12   *Histoplasma capsulatum*. *Ca* EVs from distinct strains robustly inhibited yeast-to-hyphae

13   differentiation with morphological changes occurring in less than 4 hours. A minor inhibitory

14   effect was promoted by EVs from *S. cerevisiae* and *H. capsulatum* only after 24 hours of

15   incubation. The inhibitory effect of *Ca* EVs was promoted by a combination of lipid

16   compounds identified by gas chromatography-tandem mass spectrometry analysis as

17   sesquiterpenes, diterpenes, and fatty acids. Remarkably, *Ca* EVs were also able to reverse

18   filamentation, transforming hyphal growth to yeast forms. Transcriptomic analysis

19   demonstrated that treatment with *Ca* EVs modified the expression of more than 300 genes.

20   The most effectively upregulated pathways were related to DNA metabolism. The

21   downregulated genes were mostly associated with extracellular and adhesion proteins.

22   Finally, yeast cells treated with *Ca* EVs for 24 hours lost their agar invasive ability and were

23   avirulent when inoculated in *Galleria mellonella* larvae. In summary, our results indicate that

24   fungal EVs can profoundly modify *C. albicans* growth and regulate yeast-to-hypha

25   differentiation inhibiting biofilm formation and virulence.

4

1   **Introduction**

2   *Candida albicans* is a common colonizer of the human skin and mucosa [1–3]. However,

3   in circumstances where the epithelial barrier, the immune system and/or the microbiome are

4   compromised, this species can overgrow and cause superficial and disseminated, life-

5   threatening infections [4–6]. The ability of *C. albicans* to adapt and colonize distinct organs and

6   tissues is associated with the expression of virulence factors and fitness attributes [4]. Among

7   them, a major strategic feature that facilitates *C. albicans* to persist in different environments

8   is the capacity to switch morphological stages, a tightly regulated process developed by

9   fungal organisms called dimorphism [7].

10   Dimorphic transitions in *C. albicans* involve an extensive transcriptional

11   reprogramming (reviewed by Basso et al [5]) and an intense cell wall remodeling [8]. The three

12   morphological stages of *C. albicans* regularly found in biofilm and infected tissues are yeast,

13   pseudohypha, and hypha [9]. Regulation of morphological changes are closely linked to

14   pathogenesis. For this reason, a number of studies dealing with morphogenesis in *C. albicans*

15   have been explored and several signaling pathways regulating cell shape have been described

16   [5,9]. Different environmental stimuli can induce dimorphism in *C. albicans*. For instance,

17   yeast-to-hypha differentiation is stimulated by *N*-acetylglucosamine (GlcNAc), neutral pH,

18   serum supplementation at 37^0C, 5% CO_2, low nitrogen and amino acids, among others [8,10–13].

19   Dimorphism in *C. albicans* can be also controlled by quorum sensing (QS), a

20   mechanism of microbial communication [14,15]. Fungal QS molecules (QSM) are released in

21   culture media according to the cell density. After reaching a threshold QSM regulate genes

22   involved with virulence, biofilm formation and morphogenesis [16,17]. Farnesol, farnesoic acid,

23   and tyrosol are major morphogenesis-related QSM produced by *C. albicans* [17–19], although

24   other alcohols derived from amino acids have been also characterized [20]. Farnesol and

25   farnesoic acid prevent yeast-to-hypha differentiation with no effects on growth rates [17,21].

1 Tyrosol stimulates germ tube and hyphal formation [18]. These QSM are also able to regulate

2 biofilm formation [16,22]. Furthermore, production of QSM such as farnesol and tyrosol is also

3 described in *S. cerevisiae* and trans-species crosstalk might occur [23].

4 Since the first description of fungal extracellular vesicles (EVs) by Rodrigues et al. in

5 2007 [37], a number of studies have shown that fungal organisms use EVs as a mechanism of

6 molecular exportation [24–36]. Heterogeneous populations of EVs containing lipids, proteins,

7 polysaccharides, pigments and nucleic acids cross the cell wall outwards, reaching the

8 extracellular environment [26,27,30,32,34,37,38]. Their implication during pathological and

9 physiological processes is under investigation by a number of groups. *In vitro*, fungal EVs

10 from *Cryptococcus neoformans, C. albicans, Aspergillus flavus* and *Paracoccidioides*

11 *brasiliensis* are internalized by macrophages stimulating nitric oxide and cytokine

12 production[30,33,39,40]. EVs from *A. flavus* and *P. brasiliensis* are also able to promote M1

13 polarization [39,41]. In addition, dendritic cells treated with EVs from *C. albicans* up-regulated

14 the expression of CD86 and MHCII [30]. Fungal EVs were also used to stimulate the innate

15 immune system of *Galleria mellonella* protecting the larvae stage against a subsequent

16 infection with *C. albicans, C. neoformans* and *A. flavus* [30,39,42]. In contrast, EVs can also be

17 disease-enhancing, as demonstrated by EV exposure facilitating yeast traversal across the

18 brain blood barrier in a murine model of cryptococcosis and increasing fungal burdens and

19 lesion diameters in mice infected with *Sporothrix brasiliensis* [36,43].

20 EVs also mediate communication between fungal cells. Bielska and colleagues

21 demonstrated that EVs isolated from a virulent strain of *C. gattii* were efficiently taken up by

22 macrophages previously infected with a non-virulent strain of the same species [28]. Inside

23 phagocytes the EVs promoted a rapid intracellular fungal growth transferring virulence to the

24 non-virulent strain through a mechanism apparently dependent on intact vesicles. The

1   presence of stable RNA and proteins was also required [28]. EVs also have a critical role

2   during biofilm matrix production and drug resistance in *C. albicans* [44].

3   In this work, we demonstrate that EVs produced by *C. albicans* cells (*Ca* EVs) impact

4   yeast growth, biofilm formation, yeast-to-hypha differentiation gene expression, and

5   virulence. Our results reveal previously unknown roles of fungal EVs that will likely impact

6   the physiology and pathogenesis of *C. albicans*.

7

1   **Results**

2

3   **EVs produced by yeast forms of *C. albicans* (*Ca* EVs) stimulate the growth of yeast cells**

4   ***in vitro*.** *C. albicans* usually grows as yeast forms in RPMI media under agitation at 37 ^{0}C [45].

5   Using the *C. albicans* strain 90028, we initially investigated the direct effect of yeast form-

6   derived *Ca* EVs during yeast growth under these conditions (**Fig. 1A**). Addition of *Ca* EVs to

7   *C. albicans* cultures significantly increased growth in RPMI-MOPS media in a dose-

8   dependent fashion (**Fig. 1A, upper panel**). To rule out that the effect was not related to

9   nutrient supplementation, the yeast cells were also treated with *Ca* EVs for 24 h, centrifuged,

10   washed 3 times with PBS, enumerated, and then transferred to fresh medium. Results showed

11   growth increase in the presence of *Ca* EVs slightly but significantly higher than in the control

12   (PBS); however, no EV dose-dependence was observed after 24-h incubation (**Fig. 1A, lower**

13   **panel**). Only yeast cells were visualized during the experiment (data not shown).

14
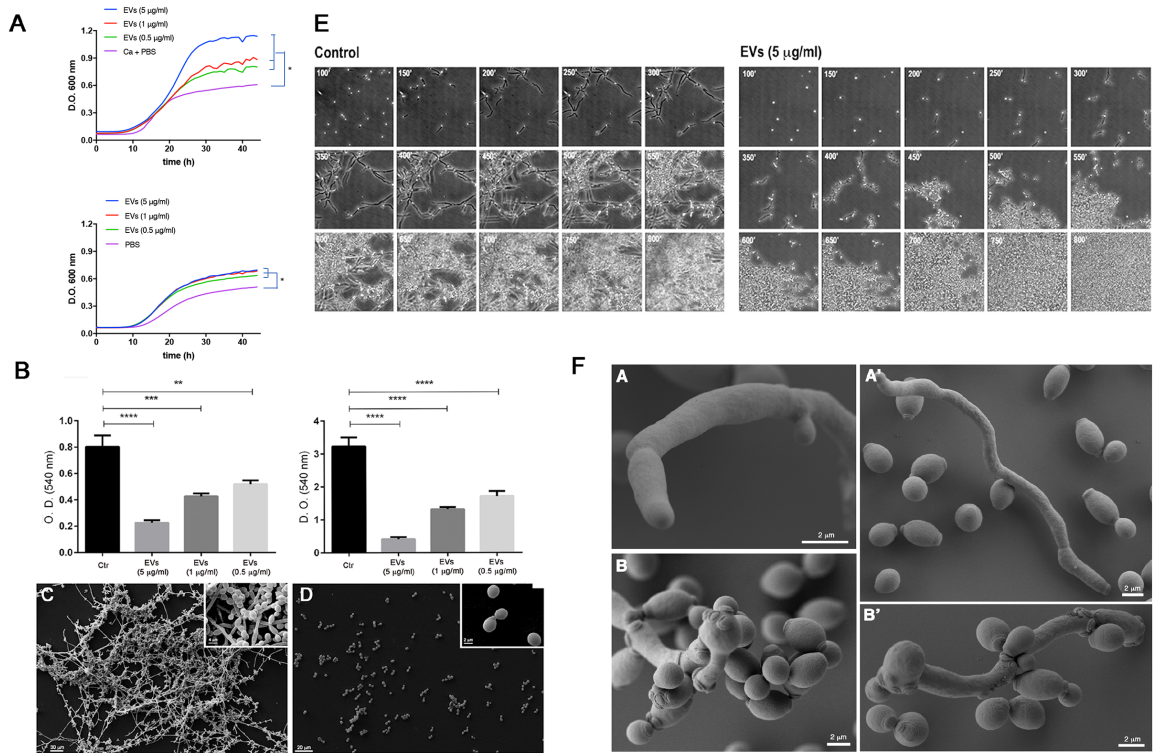
1   **Figure 1 - EVs from *C. albicans* stimulate yeast growth, inhibits biofilm formation and**

2   **yeast-to-hyphae differentiation.** Both protocols described in Methods for EV isolation were

3   used with identical results. The results presented here were obtained from *Ca* EVs isolated

4   from liquid culture medium. (A) Yeasts of *C. albicans* (90028) (10^3 yeasts) were inoculated

5   into RPMI-MOPS in the presence or absence of *Ca* EVs. Yeasts were treated with *Ca* EVs

6   (0.5, 1, or 5 µg/ml, based on sterol content). Alternatively, treated yeasts (24 h) were washed

7   and an aliquot was transferred to fresh medium. Cellular density was monitored for 72 h.

8   Data shown represent one of three consistent, biological replicates. Group comparisons were

9   submitted to one-way analysis of variance (ANOVA) with Dunnett's correction (* $p<0.0001$).

10   (B) Yeasts of *C. albicans* (90028) (10^3 yeasts) were inoculated into RPMI-MOPS in the

11   presence or absence of *Ca* EVs. Different concentrations of EVs (0.5, 1, and 5 µg/ml, based

12   on sterol content), were added to wells containing *C. albicans* yeasts (strain 90028) and cells

13   were incubated to develop biofilm for 24 and 48 h in 96-well microplates. Biofilm formation

14   was quantified by Crystal Violet method. (C) For SEM, yeasts of *C. albicans* (strain 90028),

15   untreated or treated with *Ca* EVs (5 µg/ml), were inoculated onto coverslips previously

16   coated with poly-L-lysine in RPMI-MOPS and incubated for 24 h. (D) SEM images show the

17   effect of EVs after 24 h of growth. Insets in C and D depict higher magnification of each

18   condition. Bar, 30 µm. For both experiments, the control included culture without *Ca* EV

19   addition. (E) Yeasts of *C. albicans* (90028) were inoculated into M199 medium to induce

20   filamentation in the presence or absence of *Ca* EVs (5 µg/ml, based on sterol content).

21   Cellular density was monitored, and the pictures represent the minutes of incubation (from

22   100 to 800 min). Growth under control conditions (absence of *Ca* EVs) and in the presence of

23   *Ca* EVs. The numbers indicate the time in minutes. Bar, 30 µm. (F) Yeasts of *C. albicans*

24   (90028) were inoculated into M199 medium to induce filamentation in the presence or

25   absence of EVs (5 µg/ml, based on sterol content). SEM of cells after 24 h showing the

1   hyphae and yeasts under control conditions (A and A'), and pseudohyphae with multiple

2   budding sites and yeasts (B and B').

3

4   **EVs produced by *C. albicans* inhibit biofilm formation.** Our results showed the presence

5   of yeast-derived *Ca* EVs negatively impacted biofilm formation in a dose-dependent manner

6   (**Fig. 1B**). The highest density of EVs (sterol concentration corresponding to 5 µg/ml)

7   reduced OD measurements by approximately 80-85% when compared to controls with no *Ca*

8   EV stimulation. SEM images obtained after 24 h of biofilm formation showed that the

9   negative control (biofilm formed in the absence of *Ca* EVs) exhibited a standard architecture,

10   with the presence of hypha, pseudohypha, and yeast cells attached to the coverslip (**Fig. 1C**).

11   SEM images confirmed that treatment of *C. albicans* yeast cells with EVs inhibited biofilm

12   formation. Contrasting with control conditions where the three morphological stages were

13   found, only yeast cells were visualized attached to the coverslip in the condition with EVs

14   present (**Fig. 1D**). Thus, under the conditions used in our experiments, EVs significantly

15   impaired biofilm formation in *C. albicans.*

16

17   **EVs from *C. albicans* inhibit yeast-to-hypha differentiation.** The ability to accelerate yeast

18   growth and inhibit biofilm formation suggested that *Ca* EVs could control morphogenesis in

19   *C. albicans* strain 90028. We then monitored microscopically the impact of *Ca* EVs on yeast-

20   to-hypha differentiation induced by M199 medium at 37 ^{0}C. Under control conditions

21   (absence of *Ca* EVs), the yeast cells adhered to the solid substrate (**Fig. 1E, left panel**) and

22   formed germ tubes after 1-2 h of incubation. This step was followed by true hypha formation,

23   which elongated with time. Few hyphae branching and yeast cells were visualized after 8 h,

24   but hypha represented the predominant morphological stage. The time-lapse microscopy of

25   18 h incubation is presented as a supplemental movie (**Mov. S1**). Addition of EVs to the well

10

1   drastically changed the phenotype (**Fig. 1E, right panel, and Movie S2**). Although the yeast

2   cells were able to attach to the plate and started to form germ tubes, true hypha development

3   after elongation was not observed (**Fig. 1E, right panel, and Movie S2**). In contrast, the

4   appearance of constrictions on elongated cells suggested the development of pseudohyphae

5   after 4-7 h. In addition, the cells lost their ability to adhere to the well after 6 h of incubation

6   (**Movie S2**). Multiple budding points, potentially related to a faster growth, were observed

7   along the pseudohyphae and after 24 h only yeast cells were detected in the presence of EVs

8   (**Figs. 1E, right panel, and Fig. 1F**). Long pseudohyphal filaments with yeast cells clusters

9   were observed, including a large number of yeast cells derived from pseudohyphae (**Fig 1E,**

10   **right panel**). Furthermore, there was no indication of cytotoxicity under these conditions

11   since all the yeast cells were able to grow (**Movie S2**). SEM images show the ultrastructural

12   details of pseudohyphae after EV addition. Multiple budding yeasts and several bud scars

13   were observed, when compared to hyphae in control condition (no *Ca* EV addition) (**Fig 1F**).

14   This phenomenon of yeast induction occurred in a dose-dependent manner. A minimum

15   density of *Ca* EVs, equivalent to 0.3-0.6 µg sterol/ml, was required to inhibit morphogenesis

16   at least partially (**Fig. 2A**). However, the inhibitory activity was not dependent on the number

17   of yeast cells, since different cell suspensions (1.5×10^3 to 3.5×10^4 yeast cells/well) were

18   similarly affected using the same density (5 µg sterol/ml) of EVs (data not shown).

19   Remarkably, a single treatment with EVs was sufficient to inhibit the yeast-to-hypha

20   differentiation for at least 72 h (**Fig. 2B**). Aliquots of pre-treated yeast cells (2.5×10^3 yeast

21   cells/well) were washed in PBS and plated onto fresh M199 medium and accompanied

22   microscopically for 24 h and then transferred again to fresh medium. This process was

23   repeated three times and aliquots from 48 and 72 h were added to fresh M199 medium for

24   microscopic monitoring. Regular hypha formation similar to control conditions was observed

25   only after the 96 h.

1
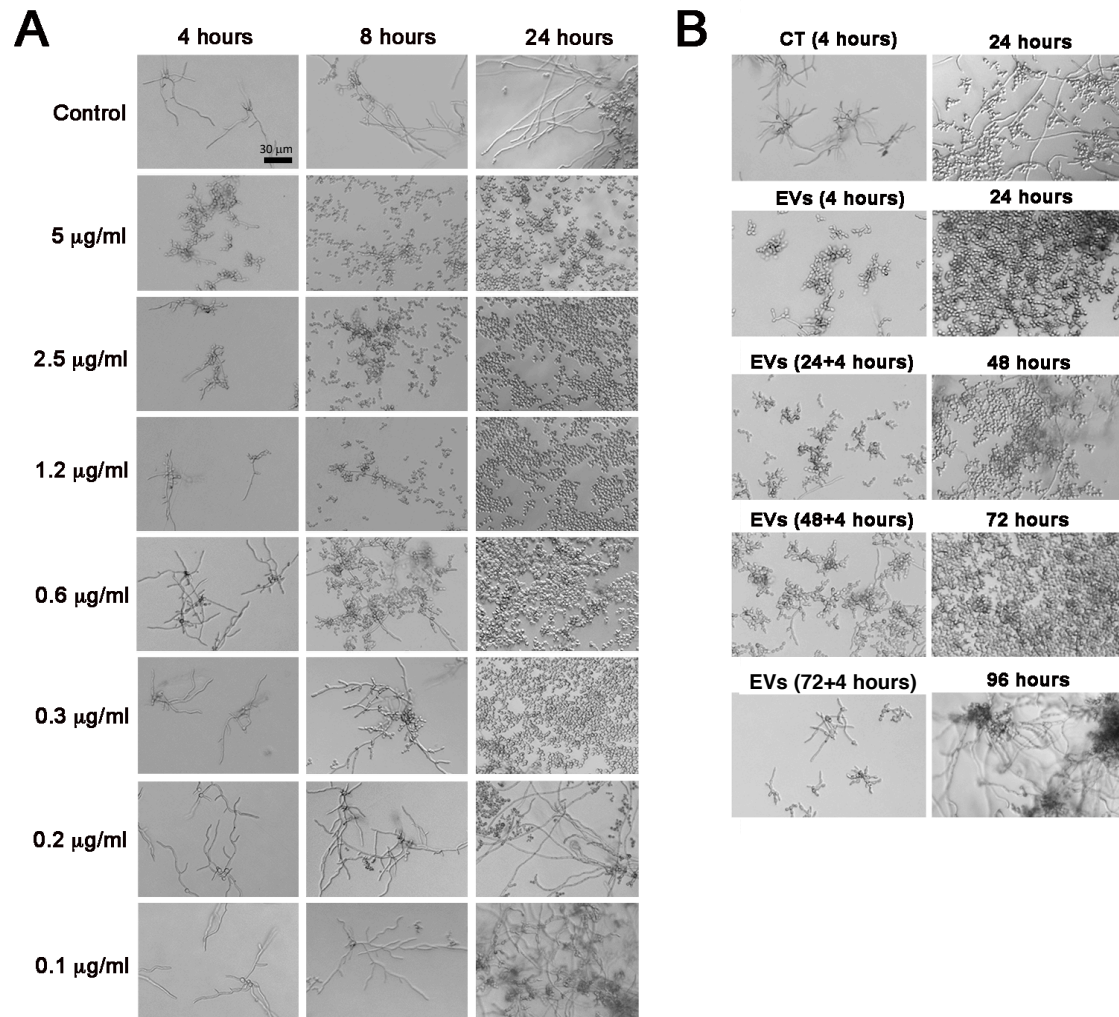
Figure 2 - The inhibitory effect of EVs from *C. albicans* (strain 90028) on yeast-to-hypha

conditions is dose-dependent and has a long-term effect. (A) Yeasts of *C. albicans* (90028)

were inoculated into M199 (pH 7) in the presence or absence of *Ca* EVs in different

concentrations (equivalent to 0.1, 0.2, 0.3, 0.6, 1, 1.2, 2.5, and 5 μg sterol/ml). Bar, 30 μm.

(B) The inhibitory effect of a single *Ca* EV treatment was tested after 24, 48, 72, and 96 h.

Aliquots of pre-treated yeasts were transferred to fresh M199 medium each 24 hours of

incubation and the differentiation accompanied microscopically. Bar, 30 μm. Experiments

were performed in biological triplicate with consistent results.

10

1   **General properties of EVs produced by different *C. albicans* strains.** EVs produced by

2   different species of *C. albicans* were isolated from culture supernatants and compared using

3   nanoparticle tracking analysis (NTA), as described [46]. The size distribution of the EVs

4   produced by *C. albicans* strains used in this work ranged from 100 to 500 nm (**Fig. 3A, B**

5   **and C**), similar to measurements published for EVs released by *C. albicans* and other fungal

6   species [30,46]. EVs released by strains SC5342 and 10231 were comparable to each other,

7   ranging from 100 to 400 nm (**Fig. 3A and C**). EVs produced by strain 90028 were also

8   mainly composed by smaller particles, ranging between 100 to 250 nm, but also depicted

9   minor populations between 300-350 nm and 420-480 nm (**Fig. 3B**). Considering that the *C.*

10   *albicans* strains release EVs with distinct average size, we normalized our experiments using

11   the total content of sterol in each vesicle preparation, as used in previous studies from our

12   group and other laboratories [30,33]. The method is highly reproducible and requires small

13   amounts of samples.

13

1

2
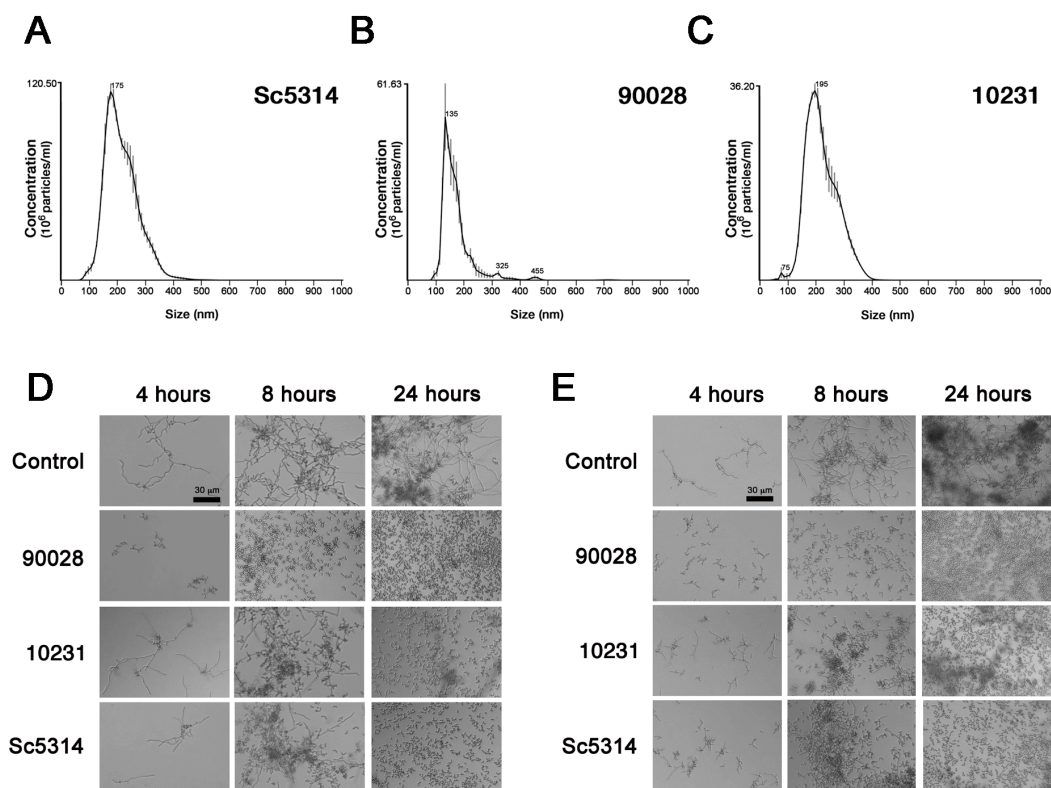
3   **Figure 3 - EVs from different *C. albicans* strains inhibit yeast-to-hyphae transition of**

4   **strains 90028 and 10231.** NTA profile of EVs produced by *C. albicans* strains (A) SC5314,

5   (B) 90028, and (C) 10231 showed similar properties of EVs. Yeasts of *C. albicans* strains (D)

6   90028 and (E) 10231 were inoculated into M199 (pH 7) in the presence or absence of *Ca*

7   EVs (equivalent to 5 µg sterol/ml) from distinct strains of *C. albicans* (90028, 10231 and

8   SC5314). Effect was visualized after 4, 8 and 24 h. PBS was added alone as a control. Bar, 30

9   µm. Experiments were performed four times with consistent results.

10

11   **The ability of EVs to inhibit yeast-to-hypha differentiation is reproducible in other**

12   **strains of *C. albicans*.** We investigated whether the ability to inhibit yeast-to-hypha

14

1   differentiation is reproducible in EVs obtained from other strains of *C. albicans*. Thus, EVs

2   were isolated from strains with distinct abilities to cause infection. For instance, strain 10231

3   is less virulent and does not produce farnesol [47]. Instead, it produces farnesoic acid, a farnesol

4   derivative at least tenfold less active in its ability to inhibit yeast-to-hypha conversion [21].

5   Strain SC5314, on the other hand, is a regular producer of farnesol [48]. The results presented in

6   **Fig. 3** show that *Ca* EVs from both strains were able to inhibit hypha formation of strain

7   90028. To confirm that the effect was not strain-specific, we evaluated the inhibitory effect of

8   the EVs produced by the *C. albicans* strains over strain 10231 (**Fig. 3E**). The EV-mediated

9   inhibition of filamentation was confirmed. Further experiments were performed using EVs

10   produced by the ATCC90028 strain in liquid medium. Although the recovery of EVs are

11   similar using solid or liquid medium (average of 0.16 and 0.18 μg of sterol/10^9 cells,

12   respectively), resulting therefore in better yields of EV.

13

14   **EV molecules with yeast-to-hypha inhibitory activity are thermo-resistant and enriched**

15   **in preparations containing non-polar lipids.** The ability to prevent yeast-to-hypha

16   differentiation was preserved by *Ca* EVs after heating them at 90 ^{0}C for 15 min (**Fig. 4A**),

17   suggesting that thermo-resistant molecules could be mediating the inhibitory effect. Since

18   lipids seem to be involved with *C. albicans* morphogenesis [16,19], we extracted and partially

19   fractioned the lipid components carried by *Ca* EVs and tested their inhibitory activity. The

20   crude lipid was partitioned using standardized protocols to enrich lipids according to their

21   polarity [49], and the organic (lower and upper) phases were added to yeast suspensions in

22   M199 medium for microscopic monitoring of morphogenesis. The lower phase (LP) activity

23   was very similar to *Ca* EVs in its ability to inhibit differentiation (**Fig. 4B**). Although the

24   upper phase (UP) was also active, its effect was observed only after 24 h of incubation. The

25   precipitate (protein-rich fraction, PF) obtained from *Ca* EV lipid extraction, likely rich in

15

1   proteins, had no apparent influence on morphogenesis (**Fig. 4B**). The LP of lipids extracted

2   from the whole cells were also able to inhibit *C. albicans* differentiation (data not shown). LP

3   obtained from liquid Sabouraud using the same extraction and partition protocol showed no

4   activity (data not shown).

5   To investigate whether the inhibitory effect of *Ca* EVs was not due to co-isolated

6   contaminants, we fractioned our bioactive samples using size-exclusion chromatography

7   (SEC), in a Sepharose CL-4B column. A single peak (fractions 8-10) containing proteins and

8   lipids was observed (**Fig. S1**). DLS analysis confirmed the presence of EVs in fraction 8,

9   corresponding to the most concentrated sample with higher amounts of lipids and proteins,

10   but not in the adjacent ones. Two populations were characterized with average sizes

11   previously reported in our studies[30], ranging from 50-120 and 240-350 nm, and possibly

12   corresponding to exosomes and ectosomes/microparticles, respectively. The inhibitory

13   activity of the lipids from each fraction was then evaluated. Fraction 8 was able to inhibit the

14   yeast-to-hypha differentiation of *C. albicans* after six hours of incubation (**Fig. S1**). Fraction

15   10, where the protein and lipid concentration were significantly reduced comparing to

16   fraction 8, displayed a behavior similar to control samples, with clear hypha formation. None

17   of the fractions where lipids and proteins were not detected showed inhibitory activity (data

18   not shown).

1
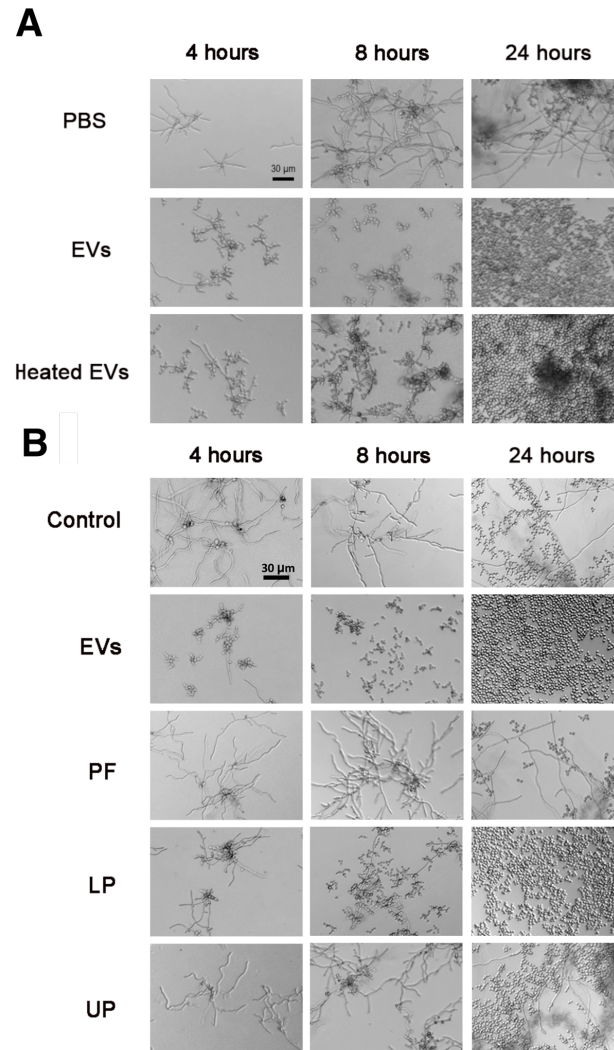
Figure 4 – Thermo-resistant molecules carried by *Ca* EVs are associated with yeast-to-hyphae inhibitory effect. (A) Yeasts of *C. albicans* (90028) were inoculated into M199 (pH 7) in the presence or absence of *Ca* EVs or heat-treated EVs in concentration equivalent to 5 μg sterol/ml. Effect was visualized after 4, 8, and 24 h. PBS was added alone as a control. Bar, 30 μm. The results shown here are representative of three independent experiments. (B) Yeasts of *C. albicans* (90028) were inoculated into M199 in the presence or absence of *Ca* EVs, EV-derived protein-rich fraction (PF), or lipid lower (LP) or upper phase (UP) in concentration equivalent to 5 μg sterol/ml. Effect was visualized after 4, 8, and 24 h. PBS was added alone as a control. Bar, 30 μm.

1 **EVs produced by other fungal species affect yeast-to-hypha differentiation in *C.***

2 ***albicans*.** On the basis of the lipid nature of the bioactive molecules studied in our work and

3 on the fact that farnesol is a QSM lipid that controls yeast-to-hypha differentiation in *C.*

4 *albicans* [16,19], we hypothesized that its presence in EVs from *C. albicans* could result in

5 filamentation inhibition. To confirm this possibility, we asked whether EVs from *S.*

6 *cerevisiae*, which synthesizes and exports farnesol in very low amounts[50], regulate

7 morphogenesis in *C. albicans*. We also included EVs from *H. capsulatum* in these analyses,

8 since farnesol has not been characterized as a lipid component in this fungus. We first

9 investigated whether the strains used in our study produced detectable amounts of farnesol

10 into the LP by reverse-phase thin-layer chromatography (RP-TLC or TLC). Whole cells were

11 used in order to obtain larger amounts of sample (**Fig. S2**). The TLC showed a sharp band in

12 the LP of *C. albicans* (*Ca*) with identical color and retention factor (R_f) obtained for a

13 farnesol (FOH) standard, strongly indicating the presence of this molecule in *C. albicans*. A

14 band with similar R_f was observed in the LP of *H. capsulatum* (*Hc*)*;* however, a distinct

15 yellowish color was visualized. Thus, a more detailed structural analysis would be necessary

16 to confirm the true nature of that band. Finally, no molecule migrating as farnesol was

17 detected in the LP from *S. cerevisiae* (*Sc*) by TLC (**Fig. S2**). Nevertheless, EVs from both

18 species were able to negatively impact *C. albicans* hyphal formation (**Fig. S3**), but the

19 kinetics of inhibition (comparing 8 h vs. 24 h of incubation time) was considerably slower

20 when compared to *Ca* EVs. With *Hc* EVs, the inhibitory effect was observed only after an

21 overnight incubation. The first signals of inhibitory effect from *Sc* EVs were detected after 8

22 h of incubation. To confirm that this was not a pleiotropic effect caused by EVs produced by

23 any of the organisms studied, we also tested the activity of EVs from murine macrophages-

24 like (MO). Contrasting with the activity of fungal EVs, MO EVs did not interfere with yeast-

25 to-hypha differentiation *in vitro* (**Fig. S3**). The fact that EVs from both *S. cerevisiae* and *H.*

1   *capsulatum* inhibited *C. albicans* differentiation, even at a lower efficacy, suggests that EV

2   molecules other than farnesol participate in the inhibitory mechanism. We next investigated

3   whether other lipids could be potentially involved in the inhibitory effect of EVs.

4

5   **Terpenes are potentially the major compounds involved with *C. albicans* yeast-to-hypha**

6   **inhibition.** To investigate whether other lipids produced by *C. albicans* could also mediate the

7   inhibitory activity of *Ca* EVs, we tested the different TLC bands from the *C. albicans* LP.

8   Using a preparative TLC plate and staining the lipids with mild iodine vapor, to avoid lipid

9   degradation, we obtained five (A-E) major fractions corresponding to separate bands (**Fig. S4**).

10 The ability of each fraction to inhibit yeast-to-hypha differentiation was investigated and only

11 the one (band A) with an R_f similar to an authentic farnesol standard showed an active effect

12 (**Fig. S4**). We then concentrated our efforts in the analysis of farnesol in fungal EVs. To that

13 end, we followed a protocol previously used for farnesol extraction [51], and employed a highly

14 sensitive GC-MS with selected-reaction monitoring (GC-MS/SRM) method, using an external

15 *bona fide* standard of farnesol. As observed in **Fig. 5A,B** (black line), the farnesol standard (at

16 4.5 picomole/µL, 1 µL injection), is comprised of a mixture of four isomers (2-*cis*,6-*cis*-

17 farnesol [Z,Z-farnesol], 2-*cis*,6-*trans*-farnesol [Z,E-farnesol], 2-*trans*,6-*cis*-farnesol [E,Z-

18 farnesol], and 2-*trans*,6-*trans*-farnesol [E,E-farnesol]), which clearly separated from each other

19 using the GC gradient conditions employed. The isomer profile was comparable to that

20 previously reported [52]. Under the experimental conditions used for the standard mixture, we

21 could detect peaks (at 9.65 and 9.81 min) with SRM transitions (not shown) and full scan

22 chromatogram elution time similar to Z,E-farnesol and E,E-farnesol isomers (peaks 3 and 5,

23 respectively) in the 90028 yeast *Ca* EV sample (**Fig. 5A,B**). **Table 1** shows the relative peak

24 intensity of these farnesol isomers and other identified compounds found in *Ca* EVs and other

25 lipid fractions. Beside the two farnesol isomers, the GC-MS analysis revealed that *Ca* EVs

1   from contain high amounts of other terpenoids or isoprenoids such as geranylgeraniol isomers,

2   and to a much lesser extent, squalene, which have not been previously reported in *C. albicans*

3   (**Table 1**). The farnesol derivative 2,3-dihydro-6-*trans*-farnesol (6, 10-dodecadienol-1-ol,

4   3,7,11 trimethyl) (peak 1) and related isoprenoid, 2,3-dihydro-6-*trans*-geraniol (6,10,14-

5   hexadecatrien-1-ol 3,7,11,15 tetramethyl) (peak 9), corresponding to farnesol and

6   geranylgeraniol units lacking a double bond at C-2, respectively, were also characterized as

7   major peaks in *Ca* EVs **(Fig. 5, Tables 1 and 2, and Fig. S7)**. Of those isoprenoids, only 2,3-

8   dihydro-6-*trans*-geraniol was also found in *Hc* and *Sc* EVs. None of the farnesol isomers or its

9   derivative (2,3-dihydro-6-*trans*-farnesol) were detected in the EVs from *H. capsulatum* and *S.*

10   *cerevisiae*, confirming that these molecules are only enriched in *Ca* EVs **(Fig. 5, Tables 1 and**

11   **2, and Fig. S7)**. Five fatty acids were also identified as major *Ca* EV components, including

12   octadecanoic (stearic acid, C18:0) and octadecenoic (oleic acid, C18:1) acids, and to a much

13   lesser extent, (9Z)-hexadec-9-enoic (palmitoleic acid, C16:2), dodecanoic (lauric acid, C12:0),

14   and tetradecanoic (myristic acid, C14:0) acids **(Fig. 5** and **Table 1)**. Fatty acids were also found

15   in EVs from *H. capsulatum* (C12:0, C14:0, and C18:0) and *S. cerevisiae* (C12:0, C14:0, C16:1,

16   C18:0, and C18:1) **(Fig. 5** and **Table 1)**. Ascorbic acid 2,6-dihexadecanoate was found in EVs

17   from the three fungal species **(Fig. 5** and **Table 1)**. This compound had no yeast-to-hypha

18   inhibitory effect (data not shown). We also characterized the major lipids found in the LP from

19   *C. albicans* and its bioactive TLC-derived band **(Fig. S4A, B)**. Equivalent amounts of 2,3-

20   dihydro-6-*trans*-farnesol and E,E-farnesol were detected in the *C. albicans* LP **(Fig. 5)**. 2,3-

21   dihydro-6-*trans*-geraniol was also identified in *Ca* LP **(Tables 1** and **2)**. Moreover, the free

22   fatty acids C12:0, C14:0, C18:0, and C18:1 were also identified in this fraction. Finally, we

23   resolved the lipids from *C. albicans* EVs by RP-TLC and the band corresponding to farnesol

24   R_f was also analyzed. We found a high similarity between the total EV lipids and this band,

25   with a clear enrichment of farnesol isomers and farnesol-like structures, and other

isoprenoids/terpenoids (**Tables 1** and **2**). In addition, we observed an enrichment of the fatty

acid C12:0 and dodecanoic acid, undecyl ester (C23:0-O2) (**Fig. 5A** and **Table 1**). Using the

standard calibration curve from the d6-E,E-farnesol isomer (**Fig. S5**), we were able to quantify

the amounts of each isoprenoid/terpenoid found in fungal EVs (**Table 2**), confirming the results

above and a significant enrichment of isoprenoids in EVs carried by *C. albicans.*
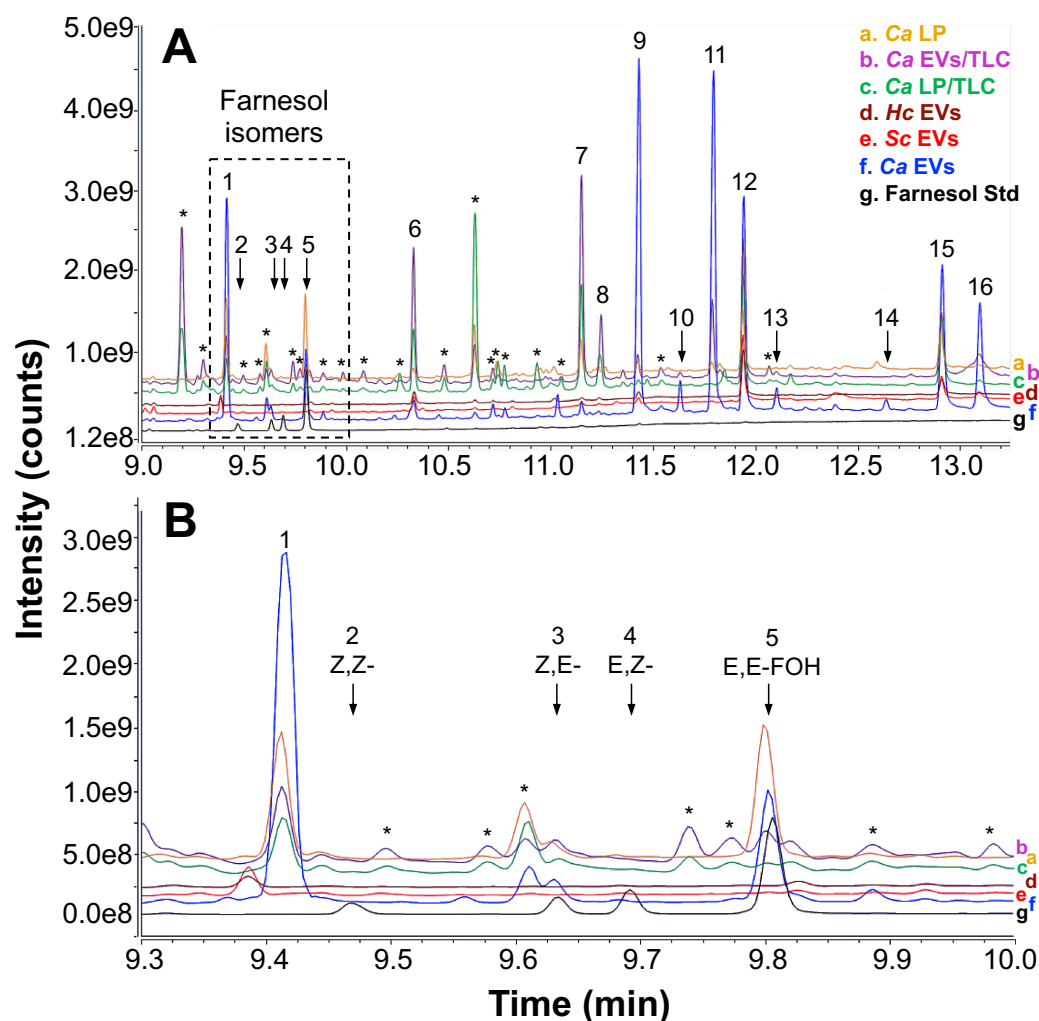
Figure 5. GC-MS analysis of fungal lipids and EVs. Lipids were extracted from *Ca* LP

fraction and EVs, and from RP-TLC band co-migrating with farnesol in those two samples.

Lipids were also extracted from *Hc* and *Sc* EVs. Resulting samples were analyzed by GC-

MS/MS. All (A) GC-MS full scan chromatogram. The chromatogram region containing the

four farnesol isomers is indicated (dashed rectangle) and shown in detail in (B). A standard

mixture containing the four farnesol isomers (Z,Z-, Z,E-, E,Z-, and E,E-FOH) was used as

21

reference (black line/trace). The GC-MS full-scan traces were overlaid and labelled (**a-g**) to facilitate visualization and comparison. Farnesol isomers and peaks of interest are indicated numerically and annotated in **Table 1**. Asterisks indicate contaminants (e.g., phthalates and other plasticizers) or compounds not identified in the library (low structural match probability).

Table 1. Major lipid compounds identified by GC-MS/MS in the lipid LP fractions and EVs of *C. albicans*, and EVs from *H. capsulatum*, and *S. cerevisiae*.

Peak number	RT (min)	Compound	Fungal Preparation/Fraction					
			C. albicans				*H. capsulatum*	*S. cerevisiae*
			LP	EVs	LP/TLC	EVs/TLC	EVs	EVs
			Peak Relative Intensity (%) [a]					
1	9.42	2,3-dihydro-6-*trans*-farnesol (6,10-dodecadien-1-ol, 3,7,11 trimethyl)	93	63	32	25	nd	nd
2	9.47	2,6-*cis*-farnesol (Z,Z-farnesol)	nd	nd	nd	nd	nd	nd
3	9.63	2-*cis*,6-*tran*s-farnesol (Z,E-farnesol)	nd	4	nd	7	nd	nd
4	9.68	2-*trans*,6-cis-farnesol (E,Z-farnesol)	nd	nd	nd	nd	nd	nd
5	9.81	2,6-*trans*-farnesol (E,E-farnesol)	**100**	20	5	9	nd	nd
6	10.33	dodecanoic acid (lauric acid, C12:0)	14	5	57	67	25	23
7	11.15	tetradecanoic acid (myristic acid, C14:0)	41	4	97	**100**	6	4
8	11.25	dodecanoic acid, undecyl ester (C23:0-O2)	nd	nd	30	32	6	4
9	11.42	2,3-dihydro-6-*trans*-geraniol (6,10,14-hexadecatrien-1-ol 3,7,11,15 tetramethyl)	14	**100**	8	12	19	9
10	11.63	geranylgeraniol (isomer 1) [c]	nd	9	nd	3	nd	nd
11	11.79	geranylgeraniol (isomer 2) [d]	10	97	nd	39	nd	nd
12	11.93	ascorbic acid 2,6-dihexadecanoate	72	60	**100**	68	**100**	**100**
13	12.11	(9Z)-hexadec-9-enoic acid (palmitoleic acid, C16:2)	nd	7	3	3	nd	4
14	12.64	squalene	nd	3	nd	nd	nd	nd
15	12.92	octadecanoic acid (stearic acid, C18:0)	41	41	62	30	38	36
16	13.12	octadecenoic acid (oleic acid, C18:1)	3	30	5	10	nd	14

[a] Not detected (below the method's limit of detecion).

[b,c] We were unable to determine the precise structures of these geranylgeraniol geometric isomers through fragmentation spectral library matching.

Table 2. Quantification of farnesol and farnesol-like structures in lipid LP fractions and EVs of *C. albicans*, and EVs from *H. capsulatum* and *S. cerevisiae*.

Fungal fraction/preparation	Farnesol isomers (ng/100 µg total lipid or protein) [a]			Farnesol-like structures (ng/100 µg total lipid or protein) [a]		
	2,3-Dihydro-6-*trans*-farnesol	Z,E-FOH	E,E-FOH	2,3-dihydro-6-*trans*-geraniol	Geranylgeraniol (isomer 1)	Geranylgeraniol (isomer 2)
Ca LP	16,3	1,8	19	2,1	nd	1,2
Ca LP/TLC	2,1	nd [b]	nd	nd	nd	nd
Ca EVs	33,7	1,6	9,7	67	4,1	63,4
Ca EVs/TLC	48,8	7,5	9,6	21	nd	77,4
Hc EVs	nd	nd	nd	4,7	nd	1,9
Sc EVs	nd	nd	nd	1,2	nd	nd

[a] LP and LP/TLC fractions were normalized by 100 µg of total lipid, whereas all EV preparations were normalized by 100 µg of protein.
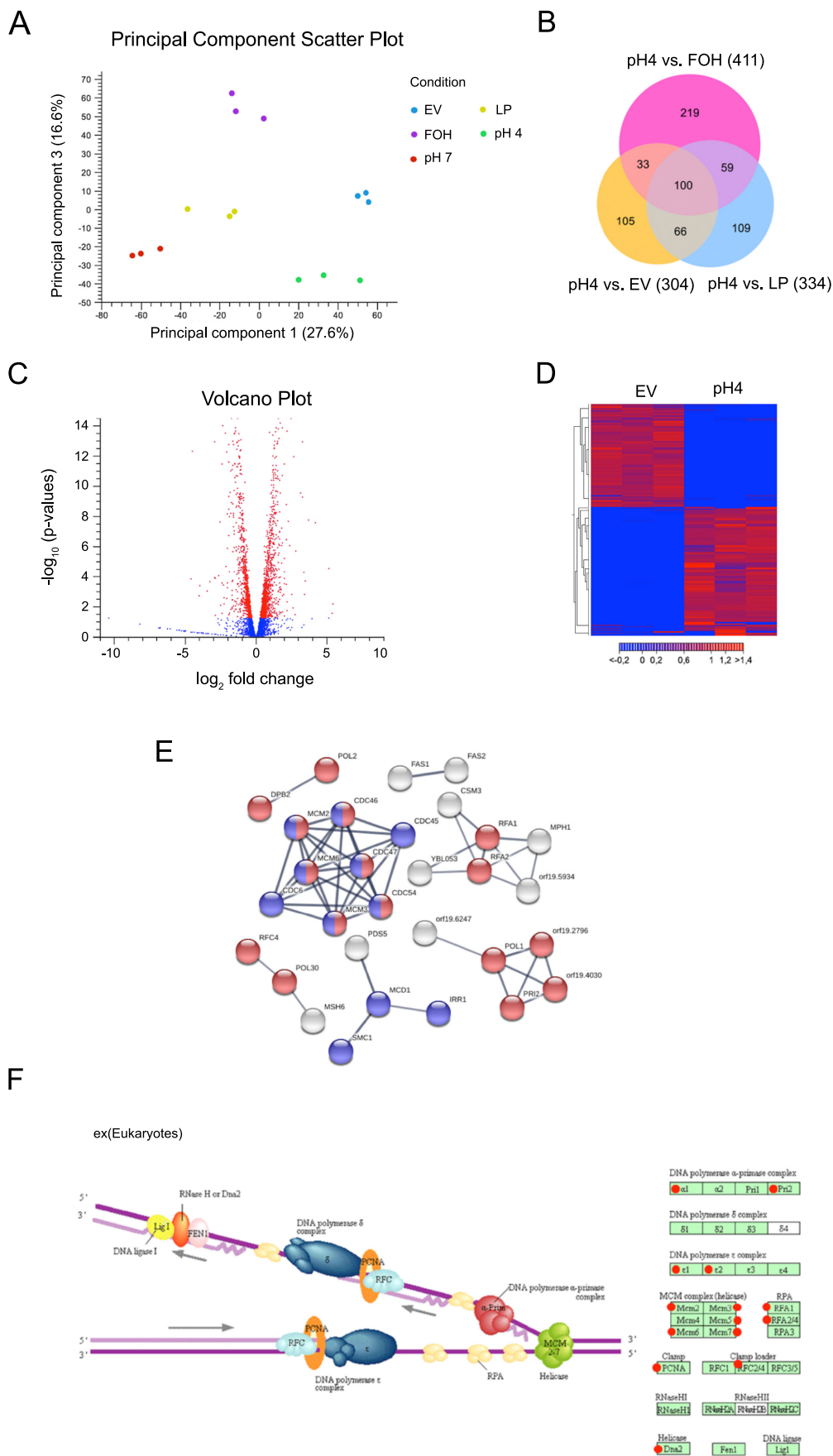[b] Not detected (below the method's limit of detection).

EVs from *C. albicans* yeast cells reverse the yeast-to-hypha differentiation and their inhibitory effect is not reversed by db-cAMP. Given the presence of additional compounds in *Ca* EVs that could potentiate their effects in morphogenesis we next investigated whether *Ca* EVs are able to reverse the yeast-to-hypha differentiation induced by M199 medium. Yeast cells were plated onto M199 medium supplemented with tyrosol for stimulation of filamentation and hyphal formation was observed after 4 h of induction (**Fig. S6**), at which time *Ca* EVs were added to the wells. Yeast cells were visualized 4 h after the addition of *Ca* EVs to the filamentous cultures, indicating that fungal EVs are able to efficiently reverse the yeast-to-hypha morphogenesis even after the highly regulated process had been initiated. As previously demonstrated [53], addition of farnesol to the wells did not reverse this effect (data not shown). Farnesol stops *C. albicans* filamentation by inhibiting adenylate cyclase (Cyr1) [54]. This effect is rescued *in vitro* by the addition of exogenous db-cAMP [55] and it was also confirmed in our experiments (data not shown). Addition of db-cAMP to yeasts pre-treated

1 with EVs did not rescue the filamentation, suggesting that the inhibitory effect was not

2 dependent on Cyr1 activity (data not shown).

3

4 **Transcriptomic alteration of *C. albicans* in response to *Ca* EV treatment.** We examined

5 the changes in *C. albicans* gene expression under filament-repressing conditions as a result of

6 *Ca* EV treatment. The cells were grown in the presence of three filament-repressing agents,

7 the *Ca* EVs and LP fraction, and standard farnesol. Control cells were maintained as yeast

8 forms at pH 4 or as filaments at pH 7. In average, we obtained at least 28 times of genome

9 coverage and more than 90% of the reads mapped to the *C. albicans* genome (**Suppl. Table**

10 **1**). We next assessed if the treatment with the filament-repressing agents would lead to

11 similar alterations in the cell transcriptome by applying a principal component analysis

12 (PCA) (**Fig. 6A**). Each condition clustered separately, indicating distinct responses. The

13 replicates clustered together, suggesting a high level of correlation between them and

14 reinforcing data reliability and the reproducibility of our results (**Fig. 6A**). When compared to

15 the control, a total of 411 mRNAs were differentially expressed in the samples treated with

16 farnesol, 334 with the LP and 304 with the *Ca* EVs (**Fig. 6B**). The complete differential

17 expression gene analysis (DEG) data are available (**Supp. Tables 2-5**). In addition, 100

18 transcripts were common to all three conditions studied (**Fig. 6B**). Analysis of the transcripts

19 altered by the EV treatment showed upregulation of 143 transcripts and 161 downregulated

20 genes (**Fig. 6C and D**). A protein interaction network analysis revealed a clear association

21 between the transcripts, as concluded from the clusters formed by the STRING (Search Tool

22 for the Retrieval of Interacting Genes) tool (**Fig. 6E**). An enrichment in DNA metabolism

23 was evident (p-value $< 1.0e^{-16}$). Gene ontology analysis identified DNA replication,

24 mismatch repair and homologous recombination as key events (**Table 3**). Fourteen transcripts

25 were linked to DNA replication (**Fig. 6F**). This result agrees with the observation that EV

1   treatment increased yeast growth rates (**Fig. 1A**). As for the comparison between the

2   transcripts affected the three filament-repressing agents, the effects induced by LP and EV

3   were more mutually related than each of them was related to the effects induced by farnesol

4   (**Table 3**). In the set of downregulated transcripts after, most of the affected transcripts were

5   related to adhesion and extracellular proteins (**Table 4**).

6

A

Principal Component Scatter Plot

Principal component 3 (16.6%)

Principal component 1 (27.6%)

Condition
- EV
- FOH
- pH 7
- LP
- pH 4

B

pH4 vs. FOH (411)

219
33
59
100
105
66
109

pH4 vs. EV (304) pH4 vs. LP (334)

C

Volcano Plot

$-\log_{10}$ (p-values)

$\log_2$ fold change

D

EV pH4

<-0,2 0 0,2 0,6 1 1,2 >1,4

E

POL2, DPB2, MCM2, CDC46, FAS1, FAS2, CSM3, CDC45, RFA1, MPH1, MCM6, CDC47, YBL053, RFA2, orf19.5934, CDC6, MCM3, CDC54, RFC4, POL30, PDS5, orf19.6247, POL1, orf19.2796, MSH6, MCD1, IRR1, PRI2, orf19.4030, SMC1

F

ex(Eukaryotes)

5'
3'
RNase H or Dna2
Lig I
FEN1
DNA ligase I
DNA polymerase δ complex
δ
PCNA
RFC
DNA polymerase α-primase complex
α-Prim
PCNA
RFC
τ
RPA
MCM 2-7
Helicase
DNA polymerase τ complex
5'
3'

DNA polymerase α-primase complex
α1 α2 Pri1 Pri2

DNA polymerase δ complex
δ1 δ2 δ3 δ4

DNA polymerase ε complex
ε1 ε2 ε3 ε4

MCM complex (helicase)
Mcm2 Mcm3
Mcm4 Mcm5
Mcm6 Mcm7

RPA
RFA1
RFA2/4
RPA3

Clamp
PCNA

Clamp loader
RFC1 RFC2/4 RFC3/5

RNaseHI
RNaseH1

RNaseHII
RNaseH2A RNaseH2B RNaseH2C

Helicase
Dna2

Fen1

DNA ligase
Lig1

1

1 **Figure 6 - Transcriptomic alterations of *C. albicans* in response to EV treatment.** (A)

2 PCA plot showing the level of correlation and reproducibility among samples: blue (*Ca* EVs),

3 purple (farnesol, FOH), yellow (*Ca* LP) and the controls: red (hyphae – pH 7) and green

4 (yeast – pH 4). (B) Venn diagram showing the transcripts that are common to and exclusive

5 to the conditions analyzed. Only transcripts that passed the statistical filter were selected for

6 the analysis (log fold change ³ 3 £ -3 and FDR adjusted p-value < 0.05). All the conditions

7 were compared to the yeast cell control (pH4). (C) Volcano plot showing the significantly

8 upregulated (left) and downregulated (right) genes during the EV treatment. The red dots are

9 all the transcripts that passed the cutoff of log fold change 3 and FDR of 0.05. (D) Heat map

10 of gene expression data during the EV treatment. The color indicates the degree of correlation

11 (red, high correlation; blue, low correlation; the scale at the bottom is represented in log

12 scale). (E) Using the STRING tool it is possible to observe the enrichment for DNA

13 replication (FDR adjusted p-value 8.4e-14) are indicated as red dots, while the cell cycle

14 (FDR adjusted p-value 4.15e-6) are indicated as blue dots, and the gray dots are proteins

15 associated to other functions. The thickness of the line indicates the degree of confidence

16 prediction of the interaction, based only in experimentally validated data. (F) KEGG analysis

17 indicated that a total of 14 genes out of 30 involved in DNA replication pathway are indicated

18 as red dots.

19

1

Table 3. Kegg Pathway enrichment - transcripts upregulated following *Ca* EV treatment.

#term ID	term description	observed gene count	background gene count	FDR
cal03030	DNA replication	16	32	0.00%
cal00240	Pyrimidine metabolism	12	67	0.00%
cal03430	Mismatch repair	8	21	0.00%
cal03410	Base excision repair	6	17	0.01%
cal03440	Homologous recombination	6	17	0.01%

Kegg Pathway enrichment - transcripts Upregulated during the LP (Lipidic Lower Phase) treatment

#term ID	term description	observed gene count	background gene count	FDR
cal03030	DNA replication	12	32	0.00%
cal04111	Cell cycle - yeast	14	85	0.00%
cal04113	Meiosis - yeast	11	71	0.01%
cal00220	Arginine biosynthesis	5	16	0.16%
cal00240	Pyrimidine metabolism	8	67	0.48%

Kegg Pathway enrichment - transcripts Upregulated during the Farnesol (FOH) treatment

#term ID	term description	observed gene count	background gene count	FDR
cal01100	Metabolic pathways	50	651	0.01%
cal01110	Biosynthesis of secondary metabolites	25	270	0.22%
cal00920	Sulfur metabolism	5	13	0.80%
cal01230	Biosynthesis of amino acids	12	99	1.15%
cal01130	Biosynthesis of antibiotics	18	200	1.31%

2

Table 4. Kegg Pathway enrichment – transcripts downregulated following *Ca* EV treatment.

#term ID	term description	observed gene count	background gene count	FDR
GO:0005576	Extracellular region	10	117	4.00%
GOTERM_BP_DIRECT	induction by symbiont of defense-related host calcium ion flux	4	24	0.15%
GOTERM_BP_DIRECT	protein metabolic process	4	33	0.20%
GOTERM_BP_DIRECT	adhesion of symbiont to host	6	70	0.19%
GOTERM_BP_DIRECT	signal peptide processing	4	89	0.39%

Treatment with EVs reduces ability of *C. albicans* to invade solid medium and decreases fungal virulence in a *Galleria mellonella* model of candidiasis. Due to the well-established connections between pathogenesis and morphological transitions in *C. albicans* [8], we investigated whether treatment with *Ca* EVs could abrogate the ability of the fungus to invade solid medium, a consequence of filamentous growth regularly correlated with virulence [56]. Colonies of *C. albicans* cultivated in M199 agar medium produced normal hypha at the edges after 5-6 days of invasive growth (**Fig. 7A, upper left panel**). In contrast, after 5-6 days no hyphae were visualized when yeast cells were pre-treated with *Ca* EVs (**Fig. 7A, upper right panel**). In fact, under *Ca* EV-treatment conditions, hyphal formation was only observed after 10-11 days of incubation (data not shown). These results were confirmed using the plate-washing method [56]. After 10 days of growth the colonies (control and EV-treated) were washed using the same flow rate, water temperature and period of time (**Fig. 7A, lower panels**), producing results that were similar to those obtained under standard conditions.

The capacity to reduce the adhesive and invasive abilities of *C. albicans* indicated that pre-incubation of yeast cells with *Ca* EVs could decrease the virulence of *C. albicans*. To investigate whether the treatment of yeast cells with EVs would impact pathogenesis we used

29

1   *G. mellonella* as a model. Infection of *G. mellonella* larvae with a lethal inoculum of yeast

2   cells of *C. albicans* cultivated in standard medium without *Ca* EVs caused melanization and

3   death in 80% of the animals in less than one week (**Fig. 7B**). Remarkably, when the pre-

4   treated yeast cells were used to infect the larvae only 10% of the animals died (**Fig. 7B**). We

5   then evaluated the ability of EVs to impair differentiation in the presence of serum, a major

6   hyphae-inducing factor in mammalian hosts[57]. Our results demonstrated that *C. albicans* EVs

7   are able to inhibit yeast-to-hypha differentiation in the presence of serum and CO_2 (data not

8   shown). Together, these data suggested that *C. albicans* EVs could directly affect the

9   pathogenesis of *C. albicans* during the infection.

10
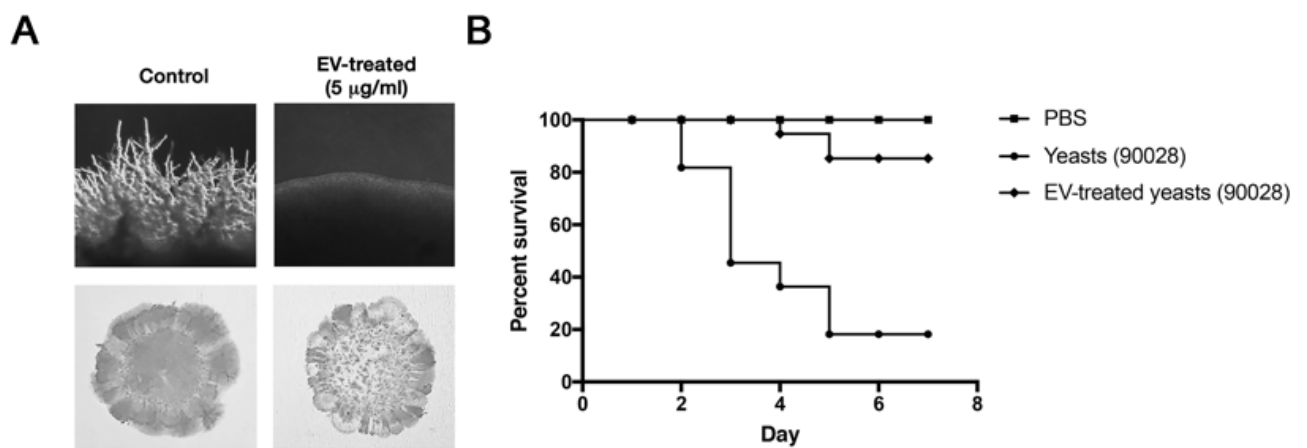
11   **Figure 7. *Ca* EVs impact invasive assay and virulence in *G. mellonella*.** (A) Yeasts of *C.*

12   *albicans* (90028) were treated with PBS (control) or *Ca* EVs in PBS (5 µg/ml) and then

13   plated onto M199 agar for 7 days. Presence of filamentation (upper panels) and agar invasion

14   (lower panel) was observed only under control conditions. (B) *Galleria mellonella* larvae

15   were infected with 10^5 yeasts of *C. albicans* untreated or pretreated with *Ca* EVs (5 µg/ml –

16   24 h) and the number of dead larvae was monitored daily. PBS indicates control larvae

17   injected with PBS. Experiments were performed in biological duplicate with similar results.

18

1   **Supplementary material (uploaded)**

2

3   **Supplemental table 1:** RNA-seq mapping statistics

4   **Supplemental table 2:** Differential gene expression analysis of the transcriptomic data from

5   the yeast cells treated with the Extracellular vesicles (EV).

6   **Supplemental table 3:** Differential gene expression analysis of the transcriptomic data from

7   the hypha cells.

8   **Supplemental table 4:** Differential gene expression analysis of the transcriptomic data from

9   the yeast cells treated with farnesol (FOH).

10   **Supplemental table 5:** Differential gene expression analysis of the transcriptomic data from

11   the yeast cells treated with the Lipidic lower phase (LP).

12   **Supplemental Figure 1:** Size-exclusion chromatography (SEC) and DLS of EVs from *C.*

13   *albicans.* The *Ca* EVs released into medium was enriched by SEC, using Sepharose CL-4B,

14   and the 500-µL fractions collected as described in Methods. Each fraction was quantified

15   according to its protein and sterol content. Fraction 8 displayed two populations of EVs with

16   effective diameters usually found in *Ca* EVs. Yeasts of *C. albicans* (90028) were inoculated

17   into M199 in the presence of each fraction to evaluate their yeast-to-hypha inhibitory activity.

18   Fractions containing EVs were normalized according to the sterol content and 5 µg/ml were

19   used. Fractions with no protein or sterol were also tested and 80% of the total content was used.

20   None of these fractions showed any inhibitory activity. Effect was visualized after 6 and 24

21   hours. PBS was added alone as a control. Bar, 30 µm.

22   **Supplemental Figure 2:** Major lipids from *C. albicans, H. capsulatum* and *S. cerevisiae*

23   resolved by TLC. LP enriched in non-polar lipids from each fungal species was obtained as

1   described in Methods. *C. albicans* (C*a*), *H. capsulatum* (*Hc*), and *S. cerevisiae* (*Sc*) lipid

2   samples were resolved by reverse-phase TLC using acetone as solvent system and stained

3   with ferric chloride-sulfuric acid reagent. Farnesol (FOH), indicated by an arrow, was used as

4   standard.

5   **Supplemental Figure 3:** Effect of EVs from different fungal species and macrophages over

6   yeast-to-hypha differentiation. Yeasts of *C. albicans* (90028) were inoculated into M199 in the

7   presence or absence of EVs from *H. capsulatum* (*Hc*), *S. cerevisiae* (*Sc*)*,* and macrophage-like

8   RAW cell line (MO) at the equivalent concentration of 5 μg sterol/ml. Effect was visualized

9   after 4, 8, and 24 h. PBS was added alone as a control (CT). Bar, 30 μm.

10   **Supplemental Figure 4:** Effects of bands isolated by preparative reverse-phase thin layer

11   chromatography (RP-TLC). (A) Lipids from LP of *C. albicans* strain 90028 (*Ca* LP) were

12   resolved by RP-TLC and the bands (a-e) stained with I_2 vapor were scraped and eluted from

13   the silica (see Methods). Farnesol (FOH), indicated by an arrow, was used as standard. (B)

14   Yeasts of *C. albicans* (90028) were inoculated into M199 in the presence or absence of each

15   eluted RP-TLC band (suspended in DMSO as described in Methods) Effect was visualized

16   after 6 and 24 h. PBS-DMSO was added alone as a control. Bar, 30 μm.

17   **Supplemental Figure 5:** Standard calibration curve of d6-farnesol E,E isomer. d6-Farnesol

18   E,E isomer (Avanti Polar) was diluted to concentrations of 0.1, 1.0, 2.5, and 5.0 ng/μL. Peak

19   areas were imported to GraphPad v9.0.0 for graph and linear regression generation. The 95%

20   confidence interval (discontinued line) of the curve is indicated.

21   **Supplemental Figure 6:** *C. albicans* EVs reversed the yeast-to-hypha differentiation. Yeasts

22   of *C. albicans* (90028) were inoculated into M199 and incubated for 4 hours to induce

23   hyphae formation. Then PBS (control), *Ca* EVs (5 μg/ml) or a combination of EVs (5 μg/ml)

24   and tyrosol (200 μM) were added to the wells. Cell morphology was visualized after 8, 12

25   and 24 hours. Bar 30 μm.

1 **Supplemental Figure 7:** Major terpenoids or isoprenoids identified in *C. albicans* EVs and

2 lipid extracts.

3 **Supplemental video 1:** *C. albicans* growth under inducing filamentous conditions. Yeasts of

4 *C. albicans* (90028) were inoculated into M199 medium to induce filamentation. Cellular

5 density was monitored up to 800 min. This video is representative of two independent

6 experiments with similar results.

7 **Supplemental video 2:** *C. albicans* growth under inducing filamentous conditions in the

8 presence of EVs. Yeasts of *C. albicans* (90028) were inoculated into M199 medium to induce

9 filamentation in the presence of EVs (5 µg/ml based on sterol content). Cellular density was

10 monitored up to 800 min. This video is representative of two independent experiments with

11 similar results.

Discussion

1   *C. albicans* morphogenesis has been associated with fungal colonization and adaptation

2 to distinct micro environmental conditions [5,6]. Additionally, morphological transition is

3 essential during biofilm formation and disease development [8,9,58,59]. In fact, inhibition of

4 morphological switching has been considered a therapeutic target for candidiasis [59].

5 Environmental and auto regulatory molecules involved with morphogenesis in *C. albicans*

6 have been extensively investigated [16,18–21]. However, the knowledge on *C. albicans* molecules

7 inducing specific morphological stages is very limited, as are the mechanisms by which these

8 compounds are released to the extracellular environment. Farnesol and tyrosol are examples

9 of QSM produced by *C. albicans* that regulate morphogenesis and biofilm formation [16,18,48,60].

10 Considering that fungal EVs have been associated with cell-cell communication and biofilm

11 matrix production [28,44], we hypothesized that these membranous compartments could be

12 involved with biofilm formation and morphogenesis of *C. albicans*. Our results demonstrate

13 that EVs released by fungi are able to directly affect yeast growth and inhibit biofilm

14 formation, through blocking of yeast-to-hypha differentiation and stimulation of hypha-to-

15 yeast differentiation.

16   The impact of EVs produced by *C. albicans* strain 90028 (*Ca* EVs) was investigated

17 during growth and biofilm formation. Remarkably, addition of *Ca* EVs to *C. albicans* yeast

18 cells culture induces faster growth. In addition, our results suggest that *Ca* EVs partially

19 mimic the effect of farnesol, displaying a filamenting-suppressing activity and inhibiting

20 biofilm formation, which could also be observed in our transcriptomic analysis. However,

21 this effect was prolonged in comparison to the activity of the commercial farnesol, indicating

22 that yeast-to-hyphae morphogenesis was temporarily turned off. Commercial farnesol

23 mixtures usually contain its four isomers (predominantly, the E,E-farnesol) and has been

24 extensively used to investigate as the QSM molecule produced by *C. albicans*. The exact

1   mechanism and signaling pathways triggered by *Ca* EVs that promote the long lasting effect

2   were not investigated, but it could involve epigenetic changes as reported previously for the

3   white-opaque transition[61]. Additional changes are also expected after *Ca* EV treatment and

4   must be further investigated. For instance, *Ca* EV-treated cells lost their ability to adhere to

5   the plate's wells after 7 h of incubation suggesting that treatment with *Ca* EVs changed

6   surface composition. Although the activity of *Ca* EVs was dose dependent, the inhibitory

7   effect was apparently not linked to yeast density in fungal cultures. These data suggest that

8   the *Ca* EV components involved with morphogenesis must reach a threshold concentration to

9   inhibit differentiation, a circumstance that is well-known for the QSM farnesol and tyrosol

10   [18,48]. This hypothesis is in agreement with the ordinary, physiological transition between yeast

11   and hyphal forms, which would not occur regularly if EVs or other extracellular regulators

12   were inhibitory at minimum concentrations. Altogether, these results indicate that *Ca* EVs

13   carry structures able to regulate growth and morphogenesis in *C. albicans*.

14   In order to confirm that *C. albicans* uses EV export as a general mechanism to control

15   yeast growth and morphogenesis *in vitro,* we isolated *Ca* EVs from two other strains with

16   distinct filamentation abilities and virulence profiles and tested their ability to inhibit yeast-

17   to-hyphae differentiation. Our data revealed that three different strains of *C. albicans* produce

18   EVs with similar properties, which were also comparable to fungal EVs, recently

19   characterized by Reis and colleagues using similar detection approaches with *C. gattii* [46]. In

20   addition, small differences in size were observed when the distinct strains were compared,

21   confirming previous data published by our group showing that *C. albicans* strains can

22   produce EVs with distinct sizes [30]. Morphological differences of EVs are usually attributed to

23   changes in composition and / or biogenesis pathways. The differentiation process of all

24   strains was affected by the *Ca* EVs. In addition, *Ca* EVs from the different strains were able

25   to promote the inhibitory effect. Thus, the *Ca* EV capacity of inhibiting yeast-to-hypha

differentiation seems to be conserved in the three strains used in our study. On the other hand, the ability of EVs isolated from different species, such as *H. capsulatum* and *S. cerevisiae,* to inhibit *C. albicans* filamentation was considerably reduced, suggesting that EVs from *C. albicans* should have a distinct cargo that influences morphogenesis.

A number of structures carried by fungal EVs could be involved with growth and morphogenesis control, including lipids, proteins and RNA. The participation of thermo-labile molecules, including a number of proteins, was discarded since the filamentation inhibition was observed even when the *Ca* EVs were heated. Since lipids are thermostable, these results suggested that a lipid compound could be responsible by the *Ca* EV-mediated inhibitory activity. Given that farnesol is a lipid that regulates morphogenesis in *C. albicans,* we speculated that this molecule could be the *Ca* EV components mediating the yeast-to-hypha inhibitory effect. Our TLC results confirmed the presence of a farnesol band with inhibitory activity exclusively in *C. albicans* lipids. However, we could not rule out that the colorimetric method used in our experiments was not sensitive to detect low amounts of farnesol in *H. capsulatum* and *S. cerevisiae* strains. In addition, it was still necessary to confirm that farnesol is addressed to *C. albicans* EVs at appropriate concentrations.

Our GC-MS results strongly indicated the presence of lipids in *C. albicans* EVs that could interfere with morphogenesis, including a family of terpenes and middle chain fatty acids[48,62,63]. Besides farnesol, other sesquiterpens and diterpenes never reported previously in *C. albicans* were the major compounds characterized in the *Ca* EVs. Of note, the proportion of the terpene species in *C. albicans* EVs was distinct from the LP that showed the highest amounts of farnesol isomers. In addition, diterpenes were found in very low amounts in EVs released by *S. cerevisiae* and *H. capsulatum* which could explain why they have a reduced activity to inhibit differentiation when compared to *Ca* EVs.

1   Our GC-MS data also showed the presence of different fatty acids species in EVs from

2   *C. albicans.* Earlier studies demonstrated that long chain fatty acids had no effect on fungal

3   differentiation, including octadecanoic an octadecenoic acids, major components in *C.*

4   *albicans* EVs[64]. However, they also showed that butyric acid was able to inhibit *C. albicans*

5   germination. Willems and colleagues[62] showed that decanoic acid inhibits *C. albicans*

6   filamentation without affecting fungal growth. In addition, Lee and colleagues[63]

7   demonstrated that C7:0, C8:0, C9:0, C10:0, C11:0 and C12:0 impacted biofilm formation and

8   filamentation. Furthermore, C7:0 and C9:0 also modified the expression of biofilm and

9   hyphal grow regulating genes. Finally, the pre-treatment of *C. albicans* with C9:0 reduced the

10   virulence of this fungus in a *C. elegans* model of candidiasis[63]. Thus, the presence of C10:0

11   and C12:0 in *C. albicans* EVs could directly contribute with filamentation inhibition.

12   Our results indicate that farnesol is not the only EV molecule regulating *C. albicans*

13   morphogenesis. Our data demonstrate that *Ca* EVs reversed the hypha formation even under

14   conditions where filamentation was already initiated and this reversion was not observed

15   when farnesol was added to the cultures in previous studies[16,50]. Remarkably, *Ca* EVs were

16   able to reverse the filamentation even when induced by M199 supplemented with tyrosol. In

17   addition, farnesol has a short time effect and is not able to modulate yeast growth

18   positively[16]. In fact, higher concentrations of farnesol completely inhibited *C. albicans*

19   growth [65]. Furthermore, addition of db-cAMP did not rescue the inhibitory effect of *Ca* EVs,

20   indicating that this inhibitory effect was independent from the adenylate cyclase activity and

21   distinct from the regulation stimulated by farnesol. Finally, according to the GC-MS analysis

22   the concentration of farnesol carried by *Ca* EVs seems to be below the limit required for its

23   activity. The concentration of farnesol usually recommended to inhibit *C. albicans*

24   differentiation is in the range of 1 to 150 μM[16,21,53,55,65]. According to our quantitative

25   analysis the sterol:protein weight ratio is 1:20 (data not shown). Most of our experiments

1   were developed using a sterol concentration of 5 μg/ml, corresponding to a protein

2   concentration of 100 μg/ml of protein. Considering the lowest concentration of farnesol used

3   in previous studies (1 μM), the amount of farnesol required for yeast-to-hyphae inhibition is

4   222.3 ng/mL. As demonstrated in **Table 2**, an EV suspension able to inhibit filamentation

5   contains approximately 11.3 ng/ml of farnesol, corresponding to the sum of both Z,E-farnesol

6   and E,E-farnesol isomers. In conclusion, *Ca* EVs carry a family of lipids, including

7   diterpenes, sesquiterpenes and fatty acids that altogether can control the morphological

8   changes in this organism. Future studies must be performed to evaluate the activity of each

9   terpene species and the combination of these structures with middle chain fatty acids to

10   inhibit *C. albicans* filamentation.

11   It has been speculated that the reduced size and round shape of yeast cells make them

12   the putative forms used by *C. albicans* to disseminate in the host. However, this possibility is

13   questionable due to the presence of serum in the blood, which would promptly induce germ

14   tube and hypha formation[57]. Our experiments show that *Ca* EVs inhibit yeast-to-hypha

15   transition even in the presence of FBS serum and 5% of CO_2, indicating that morphogenesis

16   could be controlled by EVs during mammalian infections. This possibility is corroborated by

17   the long-term effect manifested by *Ca* EVs *in vitro*. Thus, *Ca* EVs would make hypha-to-

18   yeast differentiation feasible *in vivo*, which could possibly explain how this fungus modulates

19   differentiation to disseminate.

20   It was possible to observe that the transcriptomic analysis of yeasts treated with *Ca* EVs

21   triggered a specific response in gene expression, compared to the other treatments tested. The

22   pathways upregulated were related to DNA metabolism, like the replication, mismatch repair

23   and homologous recombination. This could be associated with the higher rates of cell growth

24   observed when the cells were treated with *Ca* EVs. The EVs have been implied in cell cycle

25   or cell growth on other organisms; for example, in cancer cells, EVs can promote tumor

1   growth [66,67]. In tumor and stromal cells models, EVs are associated with cell proliferation[66].

2   In *S. cerevisiae*, EVs were recently associated with cell wall remodeling and enhancement of

3   cell viability as the EV preparations increased the viability of yeast cells in the presence of

4   caspofungin [68].

5   Based on the results discussed above, we hypothesized that pre-treatment of yeast cells

6   *in vitro* with EVs would also decrease *C. albicans'* ability to invade host cells and cause

7   disease. This possibility was reinforced by the fact that there was a delay during filamentation

8   in the edge of colonies formed by *Ca* EV-treated yeast cells during invasive agar tests. To

9   correlate the inhibitory effect of *Ca* EVs with the decrease in fungal invasion and virulence,

10   we investigated the ability of pre-treated yeast cells to kill *G. mellonella* larvae. Indeed, *Ca*

11   EV treatment significantly attenuated the ability of *C. albicans* to cause larvae death.

12   Melanization was observed only in larvae infected with untreated yeasts, confirming stress

13   due to candidiasis progress. This result indicates that by inhibiting yeast-to-hypha

14   differentiation, *Ca* EVs decrease fungal virulence. In addition, it validates the idea that

15   controlling filamentation would be a potential strategy as a therapeutic strategy[59].

16   In our study, the transcripts downregulated after *Ca* EV treatment were mainly

17   associated with adhesion to host cells. These results are possibly related to the hypovirulent

18   phenotype in the *G. mellonella* model, since a reduced ability of the fungus to adhere to host

19   cells can lead to an attenuated potential of tissue colonization. Our results can also be related

20   to models where the EVs played protective roles, including those involving *Bacillus*

21   *anthracis*, *Mycobacterium tuberculosis* or *Streptococcus pneumoniae.* In these organisms,

22   previous treatment of mice with microbial EVs favored infection control [69–71]. Our present

23   data suggest that the protective roles of EVs can include mechanisms of attenuated virulence

24   originated to an altered EV-regulated gene expression within infectious populations.

39

1   In conclusion, our results support recent findings showing that fungal EVs can be used

2   as messaging compartments and directly influence growth, biofilm production and

3   morphogenesis. The major players mediating yeast-to-hypha differentiation were

4   characterized here, and further studies are necessary to determine whether these lipids in

5   combination could be used to control candidiasis *in vivo*.

1 **Material and Methods**

2

3 **Microorganisms and culture conditions.** *C. albicans* ATCC strains 90028, 10231, SC5314

4 and the *Saccharomyces cerevisiae* strain RSY225 were cultivated in Sabouraud at 30 ^{0}C

5 under agitation (150 rpm) for 48 h. *Histoplasma capsulatum* strain G-217B (ATCC 26032)

6 was cultivated in HMM at 37 ^{0}C under agitation (180 rpm). Yeast cells of *C. albicans* were

7 washed with phosphate-buffered saline (PBS) 3 times, enumerated and then transferred to

8 medium 199 (M199) pH 4.0 or pH 7.0, RPMI-MOPS 0.165 M or RPMI supplemented with

9 10% fetal bovine serum (FBS) according to the experiments described below.

10

11 **Isolation and quantification of EVs.** EVs were isolated following protocols developed by

12 our group[30,72] with minor adjustments. Briefly, cultures (1l) from each fungal species were

13 collected after 48 h of growth as described above. Cells and debris were removed by

14 sequential centrifugation steps (4,000 and 15,000× g, 15 min, at 4 °C). An additional step of

15 filtration using a 0.45 μm membrane filter (Merck Millipore) was used to remove any

16 remaining yeast cells or debris. The supernatant was then concentrated using an Amicon

17 ultrafiltration system (100-kDa cut-off, Millipore) to a final volume of approximately 20 ml.

18 EVs were collected by centrifugation at 100 000× g for 1 h at 4 °C. Supernatant was

19 discarded and the pellet enriched in EVs was washed twice with PBS pH 7.4 at 100 000× g

20 for 1 h at 4° C. Alternatively, 300 μl containing 10^7 yeasts of *C. albicans* were plate onto

21 Petri dishes containing Sabouraud Dextrose Agar (SDA). After 24 h of growth cells were

22 harvested using a cell scraper and transferred to 20 ml of PBS. Cells and debris were

23 removed as described above, the supernatant was filtered using a 0.45 μm membrane filter

24 and the EVs were collected by centrifugation at 100 000× g for 1 h at 4 °C. To isolate EVs

25 from macrophages (RAW 264.7 macrophage-like; ATCC TIB-71) culture medium RPMI

1   supplemented with 10% FBS (400 ml) with 70% cellular confluence was collected after 24

2   hours and centrifuged (300x g and 15,000× g, 15 min, at 4 °C). The same steps of filtration

3   were used and the EVs were recovered after centrifugation at 100 000× g for 1 h at 4 °C. The

4   presence of EVs was confirmed using Dynamic Light Scattering (DLS) analysis [30] and

5   Nanotracking analysis [46]. EVs were suspended in 200 µl of PBS and aliquots of 5-10 µl were

6   used to perform the sterol quantification. Sterol content was measured using the quantitative

7   fluorometric kit 'Amplex Red Sterol Assay Kit' (Molecular Probes, Life Technologies).

8   Protein content was measured using the BCA kit (Pierce, Thermo Fisher Scientific, US).

9   Additionally, aliquots of 5-10 µl were also plated onto Sabouraud-Agar plates to confirm that

10   the preparation is sterile.

11

12   **Nanotracking analysis of *C. albicans* EVs.** Nanotracking Analysis (NTA) of fungal EVs

13   was developed on an LM10 nanoparticle analysis system, coupled with a 488-nm laser and

14   equipped with an sCMOS camera and a syringe pump (Malvern Panalytical, Malvern, United

15   Kingdom) following the conditions used by Reis and colleagues [46]. All samples were 833-

16   2,500-fold diluted in filtered PBS and measured within the optimal dilution range of

17   9×10^7 to 2.9×10^9 particles/ml. Samples were injected using a syringe pump speed of 50,

18   and three videos of 60 s were captured per sample, with the camera level set to 15, gain set to

19   3, and viscosity set to that of water (0.954 to 0.955 cP). For data analysis, the gain was set to

20   10 to 15 and the detection threshold was set to 2 to 3 for all samples. Levels of blur and

21   maximum jump distance were automatically set. The data were acquired and analyzed using

22   the NTA 3.0 software (Malvern Panalytical).

23

24   **Fungal growth and biofilm Assays.** Yeast cells of *C. albicans* (90028) were plated onto

25   polystyrene 96-well plates (10^3 yeast cells/well) containing Sabouraud or RPMI-MOPS (in

1 accordance with the CLSI standard M27 guideline) in the presence or absence of distinct

2 concentrations of EVs (0.5; 1 and 5 μg/ml, based on sterol content) and cultivated at 37 ^{0}C.

3 Cellular density was monitored for up to 48 h by measuring the culture absorbance at 600 nm

4 every 1 h using a Bioscreen C (Growth Curves USA). For Biofilm production and

5 quantification, yeast cells were plated onto polystyrene 96-well plates containing M199 (10^5

6 cells/well) in the presence of different concentrations of EVs (0.5; 1 and 5 μg/ml based on

7 sterol content). PBS was used as a negative control. Biofilm was allowed to develop for 24

8 and 48 h at 37 ^{0}C and then quantified by Crystal Violet method. Briefly, after each time point

9 the biofilm-coated wells were washed 3 times with PBS, air dried for 45 minutes and stained

10 with 0.4% aqueous crystal violet (100 μl) for 10 minutes and washed 3 times with 200 μl of

11 PBS. Then, 100 μl of absolute ethanol was added to the wells and the systems incubated for 5

12 minutes. The plate was then analyzed using a microplate reader (EL808, BioTek) at the

13 wavelength of 540 nm [73]. Tests were performed in triplicate. For Scanning Electron

14 Microscopy yeast cells were washed three times in phosphate buffered saline (PBS) pH

15 7.2 ± 0.1 to remove planktonic cells and fixed in 2.5% glutaraldehyde type I, in 0.1 M sodium

16 cacodylate buffer (pH 7.2 ± 0.1), for 1 h at room temperature. After fixation, cells were

17 washed in 0.1 M sodium cacodylate buffer (pH 7.2 ± 0.1) containing 0.2 M of sucrose and

18 2 mM of $MgCl_2$. Then, cells were dehydrated in ethanol (30, 50 and 70%, for 5 min, then

19 95% and 100% twice for 10 min), subjected to critical point drying in an EM CPD-300

20 (Leica, Wetzlar, Germany), covered with gold sputtering (10 ± 2 nm) and visualized in a

21 Zeiss Auriga 40 (Zeiss, Oberkochen, Germany) microscope operated at 2 kV.

22

23 **Yeast-to-hyphae differentiation.** Yeast cells of *C. albicans* (2.5×10^3/well) were plated onto

24 96-well plates containing the hypha-inducing media M199 or RPMI supplemented with 10%

25 Fetal Bovine Serum (FBS). To test whether the number of yeast cells would influence the

1   EVs activity different suspensions of *C. albicans* were used ($1.5x10^3$, $2x10^4$ and $3.5x10^4$ yeast

2   cells/well). Fungal EVs were added at final concentration varying from 0.025 to 5 μg/ml

3   (based on sterol content). For the lipid activity tests aliquots of 10 μl (equivalent to 5 μg/ml

4   of EVs) were added to the wells. Plates were incubated at 37 ^{0}C and 5% CO_2 for 4, 8 and 24

5   h. For each time point, the cells' morphologies were visualized under an Observer Z1

6   microscope (Carl Zeiss International, Germany) and the images were collected and processed

7   with ImageJ (NIH, US) and Photoshop (Adobe). Time-lapse video microscopies were

8   performed after plating yeast cells of *C. albicans* strain 90028 (5 x 10^3 yeast cells/well) onto

9   4-wells plate containing 1 ml of M199 medium. A final concentration of 5 μg/ml of *C.*

10   *albicans* EVs was added to the wells. PBS was used as control. Samples were placed in a

11   culture chamber with controlled temperature and CO_2 environment (37 °C and 5%,

12   respectively), attached to a Nikon Eclipse TE300 (Nikon, USA). Phase contrast images were

13   captured every minute using a Hamamatsu C2400 CCD camera (Hamamatsu, Japan)

14   connected with a SCION FG7 frame grabber (Scion Corporation, USA). Time-lapse images

15   were taken every 1 min using a Nikon Eclipse TE300 microscope attached to a Digital

16   Hamamatsu C11440-10C camera (Hamamatsu, Japan). Movies animations were generated

17   using ImageJ 1.8 software (NIH, US).

18

19   **EV Lipid extraction.** An aliquot containing 50 μg/ml of EVs were dried using a SpeedVac

20   Vacuum Concentrator (Eppendorf), followed by lipid extraction with chloroform

21   (C):methanol (M):water (W) (8:4:3; v/v/v) according to Nimrichter et al [74]. The pellet

22   containing non-extractable residues and precipitated protein was recovered by centrifugation.

23   Partition was obtained after water addition to the system to reach the proportion C:M:W

24   (8:4:5.6; v/v/v). The upper and lower phases and the protein content were dried separately

25   using SpeedVac, suspended in DMSO and their activity tested as described below. The lower

1   (LP) and upper phases (UP) contain lipids with higher and lower polarity, respectively. The

2   interphase was also dried using SpeedVac and suspended in DMSO. Aliquots of each fraction

3   (pellet, and lower and upper phases) equivalent to 5 μg/ml (based on sterol content) of EVs

4   according to previous quantification were tested. The same protocol was used to separate the

5   non-polar components of Sabouraud medium, and the lower phase was used as control.

6

7   **Thermostability of EV activity.** To investigate the thermo stability of the *C. albicans* 90028

8   yeast EV activity the samples were heated for 15 min at 90 ^{0}C. Then a final concentration

9   corresponding to 5 μg/ml (based on sterol content before heat treatment) of EVs was tested as

10   described above.

11

12   **Long-term effect of EVs.** Yeast cells of *C. albicans* (2.5×10^3/well) were plated onto 96-well

13   plates containing M199 and treated with 5 μg/ml (based on sterol content) of EVs. The *C.*

14   *albicans* cell morphology was analyzed using an Observer Z1 microscope (Carl Zeiss

15   International, Germany) after 4, 8 and 24 h. The yeast cells were collected after 24 h

16   incubation in the presence of EVs and washed three times with PBS. Yeast cells were

17   enumerated and a total of 2.5×10^3/well was transferred to fresh M199, in the absence of EVs.

18   These steps were repeated four times without addition of EVs to the cultures. Untreated yeast

19   cells cultivated in M199 were used as control each 24 h. These steps were repeated four

20   times.

21

22   **Hyphae-to-yeast differentiation.** Yeast cells of *C. albicans* (2.5×10^3/well) were plated onto

23   96-well plates containing M199 media and then incubated for 4 h to allow yeast-to-hypha

24   differentiation. After this period 100% of the yeast cells differentiated to hyphae. Then, a

25   final concentration of EVs (5 μg/ml, based on sterol content), EVs (5 μg/ml) and Tyrosol

1   (200 μM) (Sigma-Aldrich, US) were added to the wells and the morphology accompanied for

2   additional 4, 8 and 24 h as described above. PBS was used as control. Tyrosol stock was

3   diluted in methanol.

4

5   **Yeasts Lipid Extraction.** Yeast of *C. albicans, H. capsulatum* and *S. cerevisiae* (6×10^{10}

6   cells) were suspended in a mixture of C:M (2:1, v/v), stirred for 16 h at room temperature and

7   then clarified by centrifugation. Cells were reextracted with a mixture of C:M (1:2, v/v) under

8   the same conditions. Lipid extracts were combined and dried using a rotavapor (Heidolph,

9   Germany). The lipids were then suspended in a mixture of C:M:W (8:4:5.6; v/v) and

10 vigorously mixed. The lower phase was dried using a rotavapor and suspended in 2.5 ml of

11 chloroform. Aliquots were dried using Speedvac (Eppendorf, Germany) and suspended in

12 DMSO. A yeast-to-hypha differentiation assay was performed to determine the minimal

13 amount of the lower phase from *C. albicans* (20; 4; 2; 1; 0.5; 0.25; 0.125 and 0.05 mg/ml)

14 was able to block the differentiation. Aliquots of 1 mg/ml were used to the transcriptomic

15 assay.

16

17 **Size-Exclusion Chromatography (SEC).** To exclude the presence of free-contaminants in

18 EV preparations we used size-exclusion chromatography (SEC) according to Menezes-Neto

19 and colleagues [75] with minor adjustments. Briefly, Sepharose 4B (final volume of 10 mL)

20 was packed in a 10 mL syringe and then equilibrated with PBS-citrate 0.36% (w/v). The EVs

21 obtained after ultracentrifugation were suspended in a final volume of 500 μL and applied to

22 the column. A total of 30 fractions of 500 μL were collected immediately after column

23 loading using PBS-citrate as eluant. EVs aliquots of 5-10 μl were used to perform the sterol

24 and protein quantification as described previously. A yeast-to-hypha differentiation assay was

25 performed to determine the activity of each fraction. To avoid additional steps to concentrate

1 the samples the lipids from each fraction were extracted as described above and the LP

2 normalized according to the sterol content. A final concentration of 5 μg/mL of sterol was

3 used. For the fractions where sterol was not detected 400 μL of each fraction was used for

4 lipid extraction and solvent partition. The LP was dried down in a speed vac and suspended

5 in 2 μL of DMSO. An aliquot of 1 μL was used to test the inhibitory activity.

6

7 **Reverse-phase thin-layer chromatography (RP-TLC).** EVs or LP lipids were suspended in

8 C:M (1:1, v/v) and their concentration normalized by sterol content or the total weight,

9 respectively. Aliquots of 10 μL were spotted into reverse-phase TLC (RP-TLC) plates (silica

10 gel 60, RP-18, $F_{254}s$, 1 mm, Merck, Germany). The plates were developed in chambers pre-

11 saturated for 10 min using acetone as a solvent system. After development, plates were dried

12 at room temperature and the bands were visualized after spraying with a solution of 50 mg

13 ferric chloride ($FeCl_3$) in a mixture of 90 ml water, 5 ml acetic acid, and 5 ml sulfuric acid[76].

14 After spraying, plates were heated at 100 °C for 3 to 5 min. Farnesol was used as standard.

15 Under these conditions, farnesol appears as a purple band. Alternatively, the developed plates

16 were incubated in a saturated iodine chamber where the lipids appear as yellow bands. The

17 bands were scraped from the TLC and placed into microcentrifuge tubes. Lipids were

18 suspended in C:M (1:1, v/v), filtered using a PVDF membrane with 0.22 μm to a new

19 microcentrifuge tube. Samples were dried down using a speed vac, suspended in DMSO and

20 normalized by lipid weight. For the lipid activity tests aliquots of 10 μl (equivalent to 5 μg/ml

21 of EVs) were added to the wells containing yeasts of *C. albicans* in M199 medium. Plates

22 were incubated at 37 ^{0}C and 5% CO_2 for 4, 8 and 24 h. For each time point, the cells'

23 morphologies were visualized under an Observer Z1 microscope (Carl Zeiss International,

24 Germany) and the images were collected and processed with ImageJ (NIH, US) and

25 Photoshop (Adobe).

1

2 **Agar invasion assay.** Hyphal growth was stimulated using M199 medium. Yeast cells of *C.*

3 *albicans* (90028) were treated or not with EVs (5 μg/ml, based on sterol content) overnight

4 and a suspension of yeast cells 10 μl containing 10^5 cells was plated onto M199 Agar plates.

5 Plates were then incubated at 37 ^{0}C and growth was monitored daily for hypha formation.

6 After 10 days of incubation colonies were washed in a stream of water using the same flow

7 rate, water temperature and period of time as described by Cullen[56]. Colony images were

8 taken with an Optiphase microscope coupled with a digital camera (AmScope , US) and

9 processed using Adobe Photoshop.

10

11 **Farnesol extraction.** The *C. albicans* yeast 90028 EV sample (19.1 μg total sterol) was

12 resuspended in 400 μl methanol (HPLC grade, Fisher Scientific), vortexed for 2 min and

13 centrifuged for 15 min, at 14,000 x g, at room temperature. The supernatants were transferred

14 to a 2-mL PTFE-lined cap glass tube (Supelco, Cat#27134, Sigma-Aldrich). The ensuing

15 pellet was redisolved in 400 μl methanol and the previous steps were repeated. The two

16 resulting supernatants were pooled and dried under nitrogen gas in Supelco PTFE-lined cap

17 glass vials. For farnesol extraction, the yeast 90028 EV sample was partitioned by adding 500

18 μL HPLC-grade water (Fisher Scientific) and 500 μL ethyl acetate (Sigma-Aldrich, cat #

19 270989) and vortexed for 2 min. After phase separation, the upper (organic) phase was

20 collected, transferred to a fresh PTFE-lined cap glass vial, and dried under nitrogen gas.

21 Samples were then redisolved in 20 μL methylene chloride (Optima grade, Fisher Scientific),

22 transferred to Verex PTFE-lined/silicone cap vials (Phenomenex, μVial, i3 Qsert), just prior

23 to gas chromatography-mass spectrometry (GC-MS) analysis.

24

25 **Farnesol analysis by GC-MS**

1   A standard of farnesol isomer mixture (catalog # 93547, Supelco, Sigma-Aldrich) was diluted

2   in methylene chloride (Optima grade, Fisher Scientific) to a concentration of 22.5

3   picomole/µL to determine the transition ions to be used in the single-reaction monitoring

4   (SRM) method. Chromatographic separation was performed by injecting 1 µl of farnesol

5   standard onto a Thermo TSQ™ 9000 Triple Quadrupole GC-MS/MS System (Thermo

6   Scientific) set to splitless, MS transfer line at 250°C, with an AI/AS1310 series autosampler

7   (Thermo Scientific), equipped with a Zebron (ZB-FFAP, 30 m x 0.32 mm x 0.25 µm)

8   column, previously indicated for separation of farnesol isomers [52]. Initially, a full scan was

9   run to determine retention time (RT) and underivatized farnesol limits of detection, prior to

10   farnesol SRM confirmation and full scan analysis.

11   The lowest detectable level of underivatized farnesol isomers from the standard, using

12   the automated SRM (AutoSRM) mode on the TSQ 9000 Triple Quadrupole MS (Thermo

13   Scientific) with an electron ionization (EI) source temperature at 200°C, was 0.0045

14   picomole/µL. However, subsequent analyses were performed with a concentration of farnesol

15   standard of 4.5 picomole/µL, in which the detection of all four isomers (Z,Z, Z,E, E,Z, and

16   E,E) of farnesol was reproducible, and the signal of the least abundant isomer (Z,Z) was at

17   least ~10% of the most abundant isomer (E,E) and ~6-fold higher than the background. Using

18   the AutoSRM mode on the TSQ 9000 dashboard feature, the ion fragmentation was

19   optimized at their respective RT with the top 3 transition ions (81.1 to 79.1 at 8 collision

20   energy (CE), 69.1 to 41 at 6 CE, and 41.1 to 39.1 at 8 CE) were chosen and imported into

21   Chromeleon v7.2.9. Images of the SRM chromatograms of the farnesol standard and the

22   sample extracted from *C. albicans* yeast 90028 EVs were transferred from Chromeleon and

23   PowerPoint for figure generation.

24

25   **Quantitative farnesol and farnesol-like molecules by GC-MS**

1   Farnesol quantitation was measured by building a standard curve with d6-E,E-farnesol

2   (catalog # SKU700294O, Avanti Polar Lipids, Alabaster, AL) at concentrations of 0.1 ng/µL,

3   1 ng/µL, 2.5 ng/µL, and 5 ng/µL. Peak areas of the standard and samples were imported into

4   GraphPad Prism 9.0.0 for formula and R^2 generation, and graph.

5

6   **RNA isolation, purification, and sequencing.** The cells were treated with EVs (5 µg/ml,

7   based on sterol content), Farnesol (FOH) (150 µM) and lipidic lower phase (LP) (1 µl) for 18

8   h and the RNA was extracted by using the mirCury cell and plant isolation kit (QIAGEN). A

9   final number of 10^8 treated cells were lysed using 500 µL of glass beads and the 600 µL of

10   the Lysis buffer provided with the kit. Three biological replicates were obtained for each

11   condition. The concentration and RNA integrity were analyzed using Qubit (Life

12   Technologies) and bioanalyzer 2100 (Agilent Technologies, CA). The RNA-seq libraries

13   were constructed using the TruSeq Stranded mRNA kit (Illumina). According to the

14   manufacture instructions. RNA sequencing was performed using an Illumina HiSeq 2500

15   equipment at the Life Sciences Core Facility (LaCTAD) from State University of Campinas

16   (UNICAMP, Brazil).

17

18   **Transcriptomic analysis.** The data analysis was performed using CLC Genomics

19   Workbench 10.0.1 (Qiagen). Quality trimming and adapter trimming were performed using

20   default parameters. Reads were mapped to the *C. albicans* strain SC5314 reference genome

21   (ASM18296v3). Differential gene expression profiling was carried out using the negative

22   binomial distribution. The false-discovery rate adjusted p-value (FDR) procedure was used

23   for multiple- hypothesis testing correction. Genes with FDR-adjusted *P* value (less than or

24   equal to 0.05) and expression fold change of more than 3 or less than 3 were considered to be

25   differentially expressed. Functional enrichment analysis was performed on the differentially

1   expressed genes to identify overrepresented Gene Ontology (GO) biological processes using

2   the CLC Genomics Workbench and the David annotation tool [77]. The enriched metabolic

3   pathways were analyzed at the Kyoto Encyclopedia of Genes and Genomes (KEGG) [78] and

4   using David annotation tool [77]. To analyze the interactions between the transcripts we used

5   the Protein-protein tool association STRING (Search Tool for the Retrieval of Interacting

6   Genes) database [79]. The parameters we used were: High confidence – minimum required of

7   0.700, interaction sources based on experiments, network edge based on confidence.

8   Data availability. The RNA sequencing data were deposited into the Sequence Read

9   Archive (SRA) database from NCBI under accession number PRJNA203278.

10

11 ***Galleria mellonella* infection.** Larvae of wax moth *G. mellonella* was used to investigate

12 virulence of EV-treated yeast cells [80]. *C. albicans* yeast cells (2.5×10^3) were treated with EVs

13 (5 µg/ml, based on sterol content) in M199 for 24 h. Yeast cells were then washed in PBS

14 and enumerated. As a control yeast cells cultivated in Sabouraud were used. A final volume

15 of 10 µl containing 2×10^5 yeast cells was injected into the last right proleg of the larvae (200-

16 300 mg each) using a Hamilton syringe. An additional control included larvae injected with

17 10 µl PBS alone. The injected larvae were kept at 37 ^{0}C and the number of deceased subjects

18 per group was monitored daily.

19

20 **Statistical analysis.** All statistical analyses were performed using GraphPad Prism 6, version

21 5.02 for Windows (GraphPad Software).

22

51

Competing Interests Statement

Dr. Maurizio Del Poeta, M.D. is a Co-Founder and Chief Scientific Officer (CSO) of MicroRid Technologies Inc.

References:

1. Kühbacher, A., Burger-Kentischer, A. & Rupp, S. Interaction of Candida Species with the Skin. *Microorganisms* **5**, 32 (2017).

2. Ranjan, A. & Dongari-Bagtzoglou, A. Tipping the Balance: C. albicans Adaptation in Polymicrobial Environments. *J. Fungi* **4**, 112 (2018).

3. Zhang, S.-L., Wang, S.-N. & Miao, C.-Y. Influence of Microbiota on Intestinal Immune System in Ulcerative Colitis and Its Intervention. *Front. Immunol.* **8**, 1674 (2017).

4. Höfs, S., Mogavero, S. & Hube, B. Interaction of Candida albicans with host cells: virulence factors, host defense, escape strategies, and the microbiota. *J. Microbiol.* **54**, 149–169 (2016).

5. Virginia Basso, Christophe d'Enfert, S. Z. & Bachellier-Bassi, and S. From Genes to Networks: The Regulatory Circuitry Controlling Candida albicans Morphogenesis. *Curr. Top. Microbiol. Immunol.* **18**, (2018).

6. Hall, R. A. Adapting to change: interactions of Candida albicans with its environment . *Future Microbiol.* **12**, 931–934 (2017).

7. Gauthier, G. M. Dimorphism in fungal pathogens of mammals, plants, and insects. *PLoS Pathog.* **11**, e1004608–e1004608 (2015).

8. Gow, N. A. R., Van De Veerdonk, F. L., Brown, A. J. P. & Netea, M. G. Candida albicans morphogenesis and host defence: Discriminating invasion from colonization. *Nat. Rev. Microbiol.* **10**, 112–122 (2012).

9. Noble, S. M. *et al.* Candida albicans cell type switches and functional plasticity in the mammalian host. **15**, 96–108 (2018).

10. Cassone A, Sullivan PA, S. M. N-acetyl-D-glucosamine-induced morphogenesis in

Candida albicans. *Microbiologica* **8**, 85–99 (1985).

11. Csank, C. *et al.* Roles of the Candida aibicans mitogen-activated protein kinase homolog, Cek1p, in hyphal development and systemic candidiasis. *Infect. Immun.* **66**, 2713–2721 (1998).

12. Maidan, M. M., Thevelein, J. M. & Van Dijck, P. Carbon source induced yeast-to-hypha transition in Candida albicans is dependent on the presence of amino acids and on the G-protein-coupled receptor Gpr1. *Biochem. Soc. Trans.* **33**, 291 LP – 293 (2005).

13. Seeley, W. W. *et al.* Fungal Adenylyl Cyclase Integrates CO2 Sensing with cAMP Signaling and Virulence. **27**, 2349–2356 (2009).

14. Padder, S. A., Prasad, R. & Shah, A. H. Quorum sensing: A less known mode of communication among fungi. *Microbiol. Res.* **210**, 51–58 (2018).

15. Mallick, E. M. & Bennett, R. J. Sensing of the Microbial Neighborhood by Candida albicans. *PLoS Pathog.* **9**, e1003661 (2013).

16. Ramage, G., Saville, S. P., Wickes, B. L. & López-Ribot, J. L. Inhibition of Candida albicans Biofilm Formation by Farnesol, a Quorum-Sensing Molecule Inhibition of Candida albicans Biofilm Formation by Farnesol , a Quorum-Sensing Molecule Downloaded from http://aem.asm.org/ on September 16 , 2013 by Danish Veterina. *Appl. Environ. Microbiol.* **68**, 5459–5463 (2002).

17. Hornby, J. M. *et al.* Quorum Sensing in the Dimorphic Fungus. *Appl. Environ. Microbiol.* **67**, 2982–2992 (2001).

18. Chen, H., Fujita, M., Feng, Q., Clardy, J. & Fink, G. R. Tyrosol is a quorum-sensing molecule in Candida albicans. *Proc. Natl. Acad. Sci.* **101**, 5048–5052 (2004).

19. Oh, K.-B., Miyazawa, H., Naito, T. & Matsuoka, H. Purification and characterization of an autoregulatory substance capable of regulating the morphological transition in

Candida albicans. *Proc. Natl. Acad. Sci.* **98**, 4664–4668 (2002).

20. Kruppa, M. Quorum sensing and Candida albicans. *Mycoses* **52**, 1–10 (2009).

21. Riekhof, W. R. & Nickerson, K. W. Quorum sensing in Candida albicans : farnesol versus farnesoic acid . *FEBS Lett.* **591**, 1637–1640 (2017).

22. Albuquerque, P. & Casadevall, A. Quorum sensing in fungi--a review. *Med. Mycol.* **50**, 337–345 (2012).

23. Muramatsu, M., Ohto, C., Obata, S., Sakuradani, E. & Shimizu, S. Alkaline pH enhances farnesol production by Saccharomyces cerevisiae. *J. Biosci. Bioeng.* **108**, 52–55 (2009).

24. Rodrigues, M. L. *et al.* Vesicular transport systems in fungi. *Future Microbiol.* **6**, (2011).

25. Rodrigues, M. L., Franzen, A. J., Nimrichter, L. & Miranda, K. Vesicular mechanisms of traffic of fungal molecules to the extracellular space. *Curr. Opin. Microbiol.* **16**, (2013).

26. Rayner, S. *et al.* Identification of small RNAs in extracellular vesicles from the commensal yeast Malassezia sympodialis. *Sci. Rep.* **7**, 1–9 (2017).

27. Vallejo, M. C. *et al.* The Pathogenic Fungus Paracoccidioides brasiliensis Exports Extracellular Vesicles Containing Highly Immunogenic α-Galactosyl Epitopes. *Eukaryot. Cell* **10**, 343–351 (2011).

28. Bielska, E. *et al.* Pathogen-derived extracellular vesicles mediate virulence in the fatal human pathogen Cryptococcus gattii. *Nat. Commun.* **9**, (2018).

29. Rodrigues, M. L. *et al. Analysis of yeast extracellular vesicles. Methods in Molecular Biology* **1459**, (2016).

30. Vargas, G. *et al.* Compositional and immunobiological analyses of extracellular vesicles released by Candida albicans. *Cell. Microbiol.* **17**, (2015).

31. Baltazar, L. M. *et al.* Concentration-dependent protein loading of extracellular vesicles released by Histoplasma capsulatum after antibody treatment and its modulatory action upon macrophages. *Sci. Rep.* **8**, (2018).

32. Nimrichter, L. *et al.* Extracellular vesicle-associated transitory cell wall components and their impact on the interaction of fungi with host cells. *Front. Microbiol.* **7**, (2016).

33. Oliveira, D. L. *et al.* Extracellular vesicles from Cryptococcus neoformans modulate macrophage functions. *Infect. Immun.* **78**, (2010).

34. Rodrigues, M. L. *et al.* Extracellular vesicles produced by Cryptococcus neoformans contain protein components associated with virulence. *Eukaryot. Cell* **7**, (2008).

35. Rodrigues, M. L., Nimrichter, L., Oliveira, D. L., Nosanchuk, J. D. & Casadevall, A. Vesicular trans-cell wall Transport in fungi: A mechanism for the delivery of virulence-associated macromolecules? *Lipid Insights* **2** 1, (2008).

36. Ikeda, M. A. K. *et al.* Extracellular Vesicles From Sporothrix brasiliensis Are an Important Virulence Factor That Induce an Increase in Fungal Burden in Experimental Sporotrichosis. *Front. Microbiol.* **9**, 2286 (2018).

37. Rodrigues, M. L. *et al.* Vesicular polysaccharide export in Cryptococcus neoformans is a eukaryotic solution to the problem of fungal trans-cell wall transport. *Eukaryot. Cell* **6**, (2007).

38. Eisenman, H. C., Frases, S., Nicola, A. M., Rodrigues, M. L. & Casadevall, A. Vesicle-associated melanization in Cryptococcus neoformans. *Microbiology* **155**, 3860–3867 (2009).

39. Brauer, V. S. *et al.* Extracellular Vesicles from Aspergillus flavus Induce M1 Polarization In Vitro. *mSphere* **5**, e00190-20 (2020).

40. da Silva, T. A., Roque-Barreira, M. C., Casadevall, A. & Almeida, F. Extracellular vesicles from Paracoccidioides brasiliensis induced M1 polarization in vitro. *Sci. Rep.*

6, 35867 (2016).

41. Da Silva, T. A., Roque-Barreira, M. C., Casadevall, A. & Almeida, F. Extracellular vesicles from Paracoccidioides brasiliensis induced M1 polarization in vitro. *Sci. Rep.* **6**, 1–10 (2016).

42. Colombo, A. C. *et al.* Cryptococcus neoformans Glucuronoxylomannan and Sterylglucoside Are Required for Host Protection in an Animal Vaccination Model. *MBio* **10**, e02909-18 (2019).

43. Huang, S. H. *et al.* Cryptococcus neoformans-Derived Microvesicles Enhance the Pathogenesis of Fungal Brain Infection. *PLoS One* **7**, (2012).

44. Mitchell, K. F. *et al.* Candida albicans biofilm–induced vesicles confer drug resistance through matrix biogenesis. *PLOS Biol.* **16**, e2006872 (2018).

45. Reyes, G. & Ghannoum, M. A. Antifungal susceptibility testing of yeasts: uses and limitations. *Drug Resist. Updat.* **3**, 14–19 (2000).

46. Reis, F. C. G. *et al.* A Novel Protocol for the Isolation of Fungal Extracellular Vesicles Reveals the Participation of a Putative Scramblase in Polysaccharide Export and Capsule Construction in Cryptococcus gattii. *mSphere* **4**, e00080-19 (2019).

47. Thewes, S. *et al.* Phenotypic screening, transcriptional profiling, and comparative genomic analysis of an invasive and non-invasive strain of Candida albicans. *BMC Microbiol.* **8**, 187 (2008).

48. Hornby, J. M. *et al.* Quorum Sensing in the Dimorphic FungusCandida albicans Is Mediated by Farnesol. *Appl. Environ. Microbiol.* **67**, 2982 LP – 2992 (2001).

49. Svennerholm, L. Fredman, P. A procedure for the quantitative isolation of brain gangliosides. *Biochim Biophys Acta.* **18**, 97–109 (1980).

50. Hock, R., Benda, I. & Schreier, P. Formation of terpenes by yeasts during alcoholic

fermentation. *Z. Lebensm. Unters. Forsch.* **179**, 450–452 (1984).

51. DeBarber, A. E., Bleyle, L. A., Roullet, J.-B. O. & Koop, D. R. ω-Hydroxylation of farnesol by mammalian cytochromes P450. *Biochim. Biophys. Acta - Mol. Cell Biol. Lipids* **1682**, 18–27 (2004).

52. Lee, H. *et al.* Characterization of (E,E)-farnesol and its fatty acid esters from anal scent glands of nutria (Myocastor coypus) by gas chromatography–mass spectrometry and gas chromatography–infrared spectrometry. *J. Chromatogr. A* **1165**, 136–143 (2007).

53. Mosel, D. D., Dumitru, R., Hornby, J. M., Atkin, A. L. & Nickerson, K. W. Farnesol concentrations required to block germ tube formation in Candida albicans in the presence and absence of serum. *Appl. Environ. Microbiol.* **71**, 4938–4940 (2005).

54. Lindsay, A. K., Deveau, A., Piispanen, A. E. & Hogan, D. A. Farnesol and Cyclic AMP Signaling Effects on the Hypha-to-Yeast Transition in Candida albicans *Eukaryot. Cell* **11**, 1219 LP – 1225 (2012).

55. Davis-Hanna, A., Piispanen, A. E., Stateva, L. I. & Hogan, D. A. Farnesol and dodecanol effects on the Candida albicans Ras1-cAMP signalling pathway and the regulation of morphogenesis. *Mol. Microbiol.* **67**, 47–62 (2008).

56. Cullen, P. J. The plate-washing assay: A simple test for filamentous growth in budding yeast. *Cold Spring Harb. Protoc.* **2015**, 168–171 (2015).

57. Mattia, E., Carruba, G., Angiolella, L. & Cassone, A. Induction of germ tube formation by N-acetyl-D-glucosamine in Candida albicans: uptake of inducer and germinative response. *J. Bacteriol.* **152**, 555 LP – 562 (1982).

58. François L. Mayer, Duncan Wilson & and Bernhard Hube. Candida albicans pathogenicity mechanisms. *Virulence* **4**, 119–128 (2013).

1   59.   Jacobsen, I. D. *et al.* Candida albicans dimorphism as a therapeutic target. *Expert Rev.*

2   *Anti. Infect. Ther.* **10**, 85–93 (2012).

3   60.   Alem, M. A. S., Oteef, M. D. Y., Flowers, T. H. & Douglas, L. J. Production of

4   Tyrosol by Candida albicans Biofilms and Its Role in Quorum

5   Sensing and Biofilm Development. *Eukaryot. Cell* **5**, 1770 LP – 1779 (2006).

6   61.   Lohse, M. B. & Johnson, A. D. Temporal anatomy of an epigenetic switch in cell

7   programming: the white-opaque transition of C. albicans. *Mol. Microbiol.* **78**, 331–343

8   (2010).

9   62.   Willems, H. M. E., Stultz, J. S., Coltrane, M. E., Fortwendel, J. P. & Peters, B. M.

10   Disparate Candida albicans Biofilm Formation in Clinical Lipid Emulsions Due to

11   Capric Acid-Mediated Inhibition. *Antimicrob. Agents Chemother.* **63**, e01394-19

12   (2019).

13   63.   Lee, J.-H., Kim, Y.-G., Khadke, S. K. & Lee, J. Antibiofilm and antifungal activities

14   of medium-chain fatty acids against Candida albicans via mimicking of the quorum-

15   sensing molecule farnesol. *Microb. Biotechnol.* (2020). doi:10.1111/1751-7915.13710

16   64.   Noverr, M. C. & Huffnagle, G. B. Regulation of Candida albicans morphogenesis by

17   fatty acid metabolites. *Infect. Immun.* **72**, 6206–6210 (2004).

18   65.   Uppuluri, P., Mekala, S. & Chaffin, W. L. Farnesol-mediated inhibition of Candida

19   albicans yeast growth and rescue by a diacylglycerol analogue. *Yeast* **24**, 681–693

20   (2007).

21   66.   Maacha, S. *et al.* Extracellular vesicles-mediated intercellular communication: Roles in

22   the tumor microenvironment and anti-cancer drug resistance. *Molecular Cancer*

23   (2019). doi:10.1186/s12943-019-0965-7

24   67.   Ruivo, C. F., Adem, B., Silva, M. & Melo, S. A. The biology of cancer exosomes:

25   Insights and new perspectives. *Cancer Research* (2017). doi:10.1158/0008-5472.CAN-

1   17-0994

2 68. Zhao, K. *et al.* Extracellular vesicles secreted by Saccharomyces cerevisiae are

3   involved in cell wall remodelling. *Commun. Biol.* (2019). doi:10.1038/s42003-019-

4   0538-8

5 69. Rivera, J. *et al.* Bacillus anthracis produces membrane-derived vesicles containing

6   biologically active toxins. *Proc Natl Acad Sci U S A* **107**, 19002–19007 (2010).

7 70. Olaya-Abril, A. *et al.* Characterization of protective extracellular membrane-derived

8   vesicles produced by Streptococcus pneumoniae. *J. Proteomics* (2014).

9   doi:10.1016/j.jprot.2014.04.023

10 71. Brown, L., Wolf, J. M., Prados-Rosales, R. & Casadevall, A. Through the wall:

11   Extracellular vesicles in Gram-positive bacteria, mycobacteria and fungi. *Nature*

12   *Reviews Microbiology* **13**, 620–630 (2015).

13 72. Reis, F. C. *et al.* A novel protocol for the isolation of fungal extracellular vesicles

14   reveals the participation of a putative scramblase in polysaccharide export and capsule

15   construction in Cryptococcus gattii. *mSphere* **4**, (2019).

16 73. Jin, Y., Yip, H. K., Samaranayake, Y. H., Yau, J. Y. & Samaranayake, L. P. Biofilm-

17   forming ability of Candida albicans is unlikely to contribute to high levels of oral yeast

18   carriage in cases of human immunodeficiency virus infection. *J. Clin. Microbiol.* **41**,

19   2961—2967 (2003).

20 74. Nimrichter, L. *et al.* E-selectin receptors on human leukocytes. *Blood* **112**, (2008).

21 75. de Menezes-Neto, A. *et al.* Size-exclusion chromatography as a stand-alone

22   methodology identifies novel markers in mass spectrometry analyses of plasma-

23   derived vesicles from healthy individuals. *J. Extracell. Vesicles* **4**, 27378 (2015).

24 76. Lowry, R. R. Ferric chloride spray detector for cholesterol and cholesteryl esters on

25   thin-layer chromatograms. *J. Lipid Res.* **9**, 397 (1968).

1   77.   Huang, da W., Sherman, B. T. & Lempicki, R. A. Systematic and integrative analysis

2   of large gene lists using DAVID bioinformatics resources. *Nat Protoc* **4**, 44–57 (2009).

3   78.   Kanehisa, M., Furumichi, M., Tanabe, M., Sato, Y. & Morishima, K. KEGG: New

4   perspectives on genomes, pathways, diseases and drugs. *Nucleic Acids Res.* (2017).

5   doi:10.1093/nar/gkw1092

6   79.   Szklarczyk, D. *et al.* STRING v11: Protein-protein association networks with

7   increased coverage, supporting functional discovery in genome-wide experimental

8   datasets. *Nucleic Acids Res.* (2019). doi:10.1093/nar/gky1131

9   80.   Fuchs, B. B. & Mylonakis, E. Using non-mammalian hosts to study fungal virulence

10   and host defense. *Curr. Opin. Microbiol.* **9**, 346–351 (2006).

11

12

13

14

15

16

17

18

19

20

21

22